Information Circular 9069

PB86-205259

Aluminum Fluxing Salts: A Critical Review of the Chemistry and Structures of Alkali Aluminum Halides

By Charles A. Sorrell, John G. Groetsch, Jr., and D. M. Soboroff

UNITED STATES DEPARTMENT OF THE INTERIOR
Donald Paul Hodel, Secretary

BUREAU OF MINES
Robert C. Horton, Director

i.b

UNIT OF MEASURE ABBREVIATIONS USED IN THIS REPORT			
Å	angstrom	h	hour
°C	degree Celsius	mol pct	mole percent
g	gram	wt pct	weight percent
g/cm^3	gram per cubic centimeter		

Library of Congress Cataloging in Publication Data:

Sorrell, Charles A

Aluminum fluxing salts.

(Bureau of Mines information circular ; 9069)

Bibliography: p. 34-37.

Supt. of Docs. no.: I 28.27: 9069.

1. Aluminum–Metallurgy. 2. Alkali aluminum halides. 3. Flux (Metallurgy). I. Groetsch, J. G. (John G.), II. Soboroff, D. M. (David M.). III. Title. IV. Series: Information circular (United States. Bureau of Mines) ; 9069.

TN295.U4 [TN775] 622s [669'.722] 85-600303

50272-101

REPORT DOCUMENTATION PAGE	1. REPORT NO. BuMines IC 9069	2.	3. Recipient's Accession No. PB86 205259/AS

4. Title and Subtitle	5. Report Date
Aluminum Fluxing Salts: A Critical Review of the Chemistry and Structures of Alkali Aluminum Halides	1986
	6.
7. Author(s) Charles A. Sorrell, John G. Groetsch, Jr., and D. M. Soboroff	8. Performing Organization Rept. No.
9. Performing Organization Name and Address U.S Bureau of Mines Avondale Research Center 4900 LaSalle Road Avondale, MD 20782	10. Project/Task/Work Unit No. 11. Contract(C) or Grant(G) No. (C) (G)
12. Sponsoring Organization Name and Address Office of Assistant Director--Minerals & Materials Research Bureau of Mines U.S. Department of the Interior Washington, DC 20241	13. Type of Report & Period Covered Information Circular 14.

15. Supplementary Notes

16. Abstract (Limit: 200 words)

This Bureau of Mines publication reviews the structural characteristics of crystalline phases and phase equilibria data for the system NaCl-KCl-$AlCl_3$-NaF-KF-AlF_3, which encompasses a large number of molten salt fluxes currently used in aluminum recycling. Its purpose is to provide guidelines for research into the relationships between molten salt compositions and their physical properties, notably vapor pressures, densities, surface tensions, and viscosities, knowledge of which is essential to maximizing fluxing efficiencies and metal recovery and minimizing hazardous emissions and disposal problems. In addition, this report describes experimental determinations of sub solidus compatibility relationships in the system, which is of the quaternary reciprocal type. containing 12 different stable 4-phase assemblages in the solid state. The compatibility diagram serves to define the important compositional planes across which important changes in properties are likely to occur.

17. Document Analysis a. Descriptors

Molten salt fluxes
Aluminum recycling
Cryolite
Aluminum halides
Alkali halides

b. Identifiers/Open-Ended Terms

Recycling
Phase equilibria
Fluxing
Metal recovery
Hazardous wastes

c. COSATI Field/Group 07B Inorganic Chemistry; 11F Metallurgy and Metallography

18. Availability Statement	19. Security Class (This Report)	21. No. of Pages
Release unlimited by NTIS.	Unclassified	44
	20. Security Class (This Page) Unclassified	22. Price

(See ANSI-Z39.18) See Instructions on Reverse OPTIONAL FORM 272 (4-77) (Formerly NTIS-35) Department of Commerce

CONTENTS

Page

ILLUSTRATIONS

ILLUSTRATIONS--Continued

TABLES

ALUMINUM FLUXING SALTS: A CRITICAL REVIEW OF THE CHEMISTRY AND STRUCTURES OF ALKALI ALUMINUM HALIDES

By Charles A. Sorrell,[1] John G. Groetsch, Jr.,[2] and D. M. Soboroff[3]

ABSTRACT

This Bureau of Mines publication reviews the structural characteristics of crystalline phases and phase equilibria data for the system $NaCl-KCl-AlCl_3-NaF-KF-AlF_3$, which encompasses a large number of molten salt fluxes currently used in aluminum recycling. Its purpose is to provide guidelines for research into the relationships between molten salt compositions and their physical properties, notably vapor pressures, densities, surface tensions, and viscosities, knowledge of which is essential to maximizing fluxing efficiencies and metal recovery and minimizing hazardous emissions and disposal problems.

In addition, this report describes experimental determinations of subsolidus compatibility relationships in the system, which is of the quaternary reciprocal type, containing 12 different stable 4-phase assemblages in the solid state. The compatibility diagram serves to define the important compositional planes across which important changes in properties are likely to occur.

[1]Geologist.
[2]Chemical engineer.
[3]Research supervisor.
Avondale Research Center, Bureau of Mines, Avondale, MD.

INTRODUCTION

This publication combines a review of technical information from the literature with experimental data associated with remelting of scrap aluminum and recycling of dross. Bureau of Mines research in this area is not new; in 1916, Gillett (16)[4] published a lengthy summary of the problem and reviewed the technology available at that time. The problems encountered in melting aluminum are consequences of its extreme reactivity, exceeded only by those of the alkali and alkaline earth metals. Were it not for the fact that a thin, transparent aluminum oxide film forms on the surface of the metal immediately on exposure to the atmosphere and serves as an effective barrier to further reaction, aluminum would find few practical applications.

During melting of scrap aluminum, formation of an oxide layer on the surface of the molten metal is unavoidable unless melting is accomplished in a high vacuum or completely inert atmosphere, neither of which is a feasible method. Reactions with the furnace atmosphere form not only aluminum oxide, Al_2O_3, but also aluminum nitride, AlN, aluminum carbide, Al_4C_3, and a range of oxide and oxynitride spinels. Fortunately, even though the densities of these phases are greater than that of molten aluminum, some remain on the surface of the melt and can be skimmed prior to removal of the melt from the furnace. This skim, or dross, can contain as much as 85 pct metallic aluminum trapped as droplets; these droplets are coated with a thin but remarkably strong layer of oxides which prevents the droplets from coalescing and combining with the metal in the bath. Larger aluminum producers sell the skim or dross to smaller, independent operators who recycle it to recover a portion of the metal content.

There are other problems with melting aluminum scrap. Because the material, which may include beverage cans, borings and turnings, foil, etc., has a high specific surface area, it oxidizes readily, and the oxide coating prevents the metal from coalescing into a pool. In practice, therefore, the scrap is added to a molten metal heel in a charging well and is pushed beneath the surface as rapidly as possible. It has become standard practice to use a cover of molten salt on the surface of the liquid metal in the charging well to serve the multiple purposes of protecting the aluminum from further oxidation, stripping the oxide film from the molten metal so the droplets can coalesce, and holding the solid particles in suspension so that a clean metal can be recovered.

The mechanisms by which the salt "flux" strips the oxide from the metal and holds the solids in suspension are not well understood. Sully (60) provided a reasonable explanation of the mechanism for suspension of solids based on the observation that 90 wt pct NaCl-10 wt pct CaF_2 molten salts loaded with 10 to 15 wt pct alumina of various types behaved as thixotrophic fluids, through which the settling velocities of solids were nearly zero. It was thought for many years that the fluxing salt dissolved the aluminum oxide from the surface of the metal, but it now appears that this is not a major factor. Phillips showed that, though the solubility of aluminum oxide in molten cryolite, Na_3AlF_6, is appreciable (45), addition of NaCl to the melt decreases the solubility to very low levels (46). It has since been suggested (65-66) that the low interfacial tension between the salt and molten aluminum is the primary cause of the stripping. Because the salt wets the metal and the oxide particles and, in turn, the metal does not wet the oxide, the stripping action is very effective. It is also believed that the presence of fluorides in the salt is beneficial in lowering the interfacial tension, enhancing the stripping action. For this reason, fluxing salts commonly are made up of chlorides with a small percentage of fluoride, normally cryolite, Na_3AlF_6, or fluorspar, CaF_2.

In the most recent review of the chemistry and properties of salt fluxes used

[4]Underlined numbers in parentheses refer to items in the list of references at the end of this report.

in secondary aluminum production processes, Rao (49) listed 122 flux compositions from the literature and 36 patented compositions, nearly all of which are mixtures of halides. The most commonly used fluxes are mixtures of NaCl and KCl in approximately equal amounts with 3 to 5 wt pct cryolite added. The chloride mixture has a melting point near the minimum liquidus temperature of ~645° C, just below the melting point of aluminum. This fact is important in the recycling of drosses in rotary kilns because, during heating of the charge, the salt melts and coats the aluminum before the metal melts and thereby protects the metal from further oxidation. The fluoride is added to enhance the fluxing action, though some operators obtain acceptable results without the fluoride. Of the 158 compositions listed by Rao, 49 are formulated from various mixtures of NaCl, KCl, $AlCl_3$, NaF, KF, and AlF_3 or from mixtures of compounds of these halides; the majority of the other compositions listed contain one or more of those six halides with small percentages of other salts.

Study of the literature indicates that no truly thorough investigation of any fluxing salt system has been done. In the case of the alkali aluminum halides, the system itself has not even been defined. Changes made in fluxing salts since 1916 have used trial and error as bases, and all the salt properties and relevant reactions have not been determined. There are abundant data on liquidus temperatures, vapor pressures, densities, surface tensions, viscosities, and reactions with ambient atmospheres for small compositional ranges within many systems, but there is no complete characterization of an entire system. In view of the fact that incongruent vaporization, reactions with the metal and the suspended solids, and hydrolysis reactions with combustion products all are likely to occur, it is reasonable to expect that molten salt compositions can vary rapidly with time over broad ranges, so it is essential that the whole chemical system be defined and characterized. This information is also necessary to facilitate development of processes for recycling or safe disposal of spent salt slags (34). Because of the wide use of compositions within the system NaCl-KCl-$AlCl_3$-NaF-KF-AlF_3 in present-day aluminum recycling, it has been selected as the first to be studied.

This report is restricted to a discussion of structures and melting characteristics, obtained from the literature, and determination of compatibility relationships based on Bureau of Mines experimental research.

CRYSTAL CHEMISTRY OF THE ALKALI ALUMINUM HALIDES

Because several researchers have shown relationships between melting and vaporization characteristics and structure of the crystalline solids, and because some of the structural characteristics of the solids have been observed in the molten state, data on the crystalline phases reported to be stable in the system NaCl-KCl-$AlCl_3$-NaF-KF-AlF_3 are assembled here. Crystallographic data for the 14 phases in the system with references for the structural descriptions are listed in table 1.

THE ALKALI HALIDES

The alkali halides--NaCl (halite, rock salt), KCl (sylvite), NaF (villiaumite), and KF--are isostructural, crystallizing in the familiar rock salt structure, space group Fm3m (No. 225), with ions located in the following positions:

$$\text{Alkali : (4a) } 000;\ \frac{1}{2}\frac{1}{2}0;\ \frac{1}{2}0\frac{1}{2};\ 0\frac{1}{2}\frac{1}{2}$$

$$\text{Halide : (4b) } \frac{1}{2}\frac{1}{2}\frac{1}{2};\ \frac{1}{2}00;\ 0\frac{1}{2}0;\ 00\frac{1}{2}$$

The alkali ions are coordinated with six halide ions on the corners of regular octahedra; conversely, the halide ions are coordinated with six alkali ions (6:6 coordination) so that each octahedron shares all eight faces with adjacent octahedra. Interionic distances, calculated from the lattice parameters in table 1, are listed in table 2. Comparison

TABLE 1. - Crystallographic data and sources of powder diffraction data for crystalline phases in the system $NaCl-KCl-AlCl_3-NaF-KF-AlF_3$

Crystalline phase	System and space group	Cell parameters[1]	Calculated density, g/cm^3	References	PDF card[2]
NaCl	Cubic, Fm3m...........	a = 5.6402	2.163	3, 61	5-628
KCl	...do.................	a = 6.2431	1.987	3, 63	4-587
NaF	...do.................	a = 4.6342	2.802	48, 63	4-793
KF	...do.................	a = 5.347	2.524	48, 63	4-726
$AlCl_3$	Monoclinic, C2/m......	a = 5.92, b = 10.22, c = 6.16, β = 108°.	2.498	28, 62	22-10
AlF_3	Rhombohedral, R32.....	a = 5.039, α = 58.5°.	3.197	27, 54, 58	9-138
	Hexagonal cell........	a = 4.927, c = 12.445.	3.197	27, 54, 58	NAp
Na_3AlF_6	Monoclinic, $P2_1/c$.....	a = 5.46, b = 5.61, c = 7.80, β = 90.18°.	2.918	35, 43, 59	25-772
K_3AlF_6	Tetragonal, I4/mmm or P4/mnc...............	a = 5.944, c = 8.468.	2.867	6, 20, 22, 59	3-615
K_2NaAlF_6	Cubic, Pa3 or Fm3m....	a = 8.1120	3.013	21, 38, 59, 62	22-1235
$Na_5Al_3F_{14}$	Tetragonal, P4/mnc....	a = 7.0142, c = 10.400.	2.997	4, 42	30-1144
$KAlF_4$	Tetragonal, P4/mmm....	a = 3.550, c = 6.139.	3.049	5, 44	2-595
$NaAlF_4$	...do.................	a = 3.48, c = 6.29.	2.746	15, 17, 24, 37	19-1243
$NaAlCl_4$	Orthorhombic, $P2_12_12_1$.	a = 10.36, b = 9.92, c = 6.21.	1.996	1, 53	23-649
$KAlCl_4$	Monoclinic, $P2_1/m$.....	a = 7.23, b = 10.48, c = 9.25, β = 93.3°.	1.973	53	23-468

Nap Not applicable.

[1]Unit cell parameters reported in angstroms at room temperature (20°-26° C).

[2]Powder Diffraction Files, compiled by the Joint Committee on Powder Diffraction Standards, International Centre for Diffraction Data, 1601 Park Lane, Swarthmore, PA 19081.

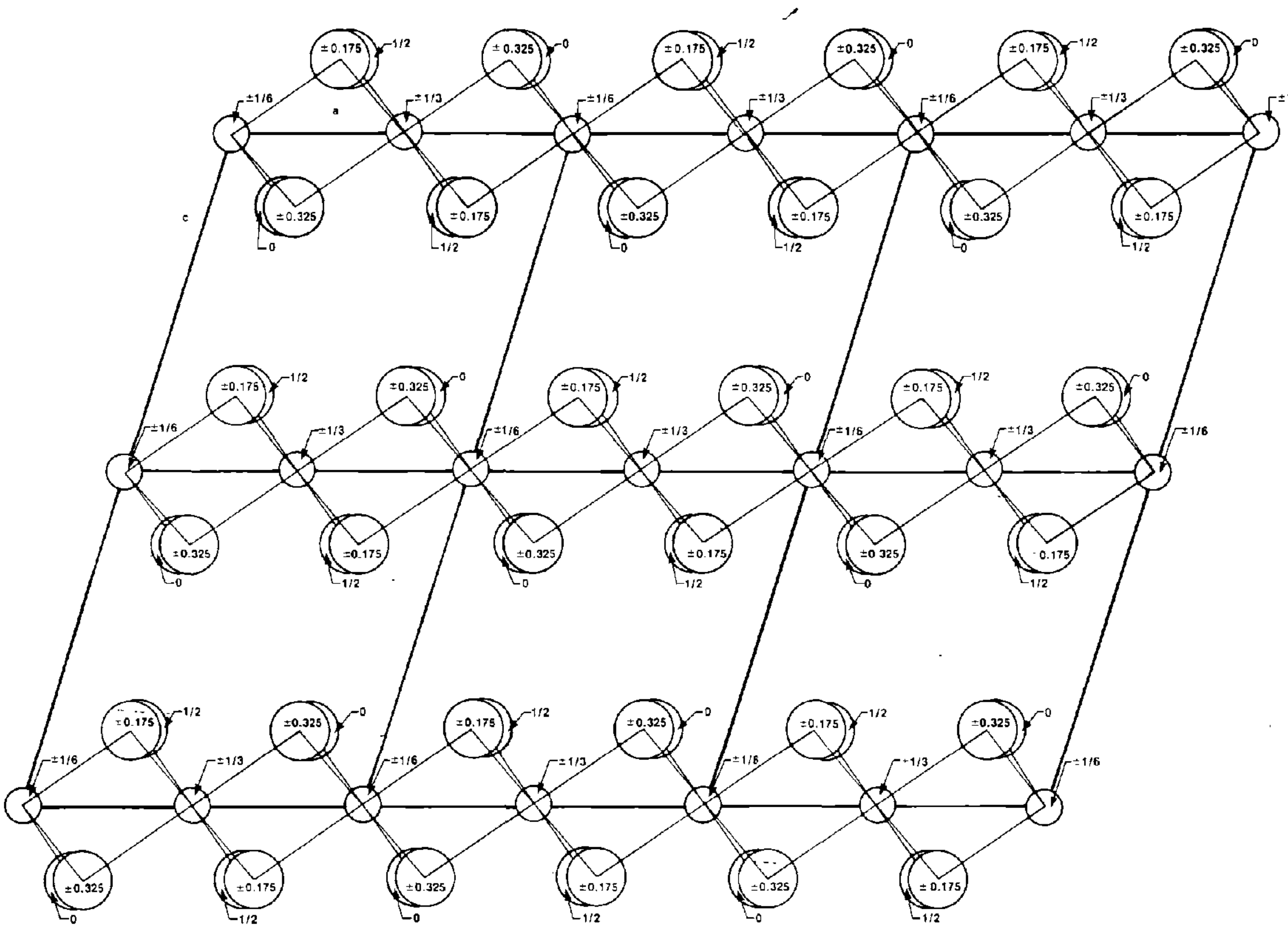

FIGURE 1. - The crystal structure of $AlCl_3$, projected on the (010) plane. Small atoms are Al; large atoms are Cl.

TABLE 2. - Measured and calculated interionic distances in the alkali halides, MX

Crystal	Measured		Calculated[1]		Crystal	Measured		Calculated[1]	
	M-X	X-X	M-X	X-X		M-X	X-X	M-X	X-X
NaCl..........	2.802	3.988	2.76	3.62	NaF...........	2.367	3.277	2.31	2.72
KCl...........	3.147	4.450	3.24	3.62	KF............	2.674	3.781	2.69	2.72

[1]Calculations were made using the following radii: Na^+, 0.95 Å; K^+, 1.33 Å; Cl^-, 1.81 Å; F^-, 1.36 Å.

of measured and calculated interionic distances shows a rather stable configuration, with the alkali-halide values near the potential minimum and little anion-anion repulsion. The alkali halides are, therefore, very stable phases, as will be shown later.

ALUMINUM CHLORIDE

The layer structure of aluminum chloride, $AlCl_3$, is shown in figures 1 and 2. The structure is monoclinic, space group C2/m (No. 12), with atoms in the following positions:

$$\text{Al} \quad : (4g) \pm \left(0y0;\ \tfrac{1}{2},\tfrac{1}{2}+y,0\right);\ y=0.167$$

$$Cl(1) : (4i) \pm \left(x0z;\ \frac{1}{2}+x,\frac{1}{2},z \right);\ x=0.226;\ z=0.219$$

$$Cl(2) : (8j) \pm \left(xyz;\ x\bar{y}z;\ \frac{1}{2}+x,\frac{1}{2}+y,z;\ \frac{1}{2}+x,\frac{1}{2}-y,z \right);$$

$$x=0.250;\ y=0.175;\ z=0.781$$

The structure consists of a distorted close-packed arrangement of chloride ions in which all the octahedral sites are empty in one layer and two-thirds of the octahedral sites are occupied by aluminum ions in adjacent layers. The layers are held together by weak van der Waals bonds. Within the bonded layers, the octahedra share all six corners with adjacent octahedra. The $AlCl_6$ octahedra are all identical, slightly distorted, with two Cl^- ions at 2.29 Å, two at 2.32 Å, and two at 2.33 Å from the Al^{3+} ion. The octahedral edges are much shorter than the sum of the anionic radii, 3.62 Å, with two Cl-Cl distances of 3.10 Å, two of 3.28 Å, and eight of 3.33 Å. This is because the radius ratio, 0.28, is too small for a stable octahedral coordination. A structure with tetrahedral coordination is not possible, however, because of the requirements of the electrostatic valence rule. The structure is, therefore, a compromise between conflicting physical requirements; the high vapor pressures and low melting point, as discussed later, are a consequence of the unstable structure. Aluminum chloride is essentially isostructural with gibbsite, $Al(OH)_3$.

ALUMINUM FLUORIDE

Unlike the layer structure of $AlCl_3$, the structure of aluminum fluoride, AlF_3, is a continuous, three-dimensional

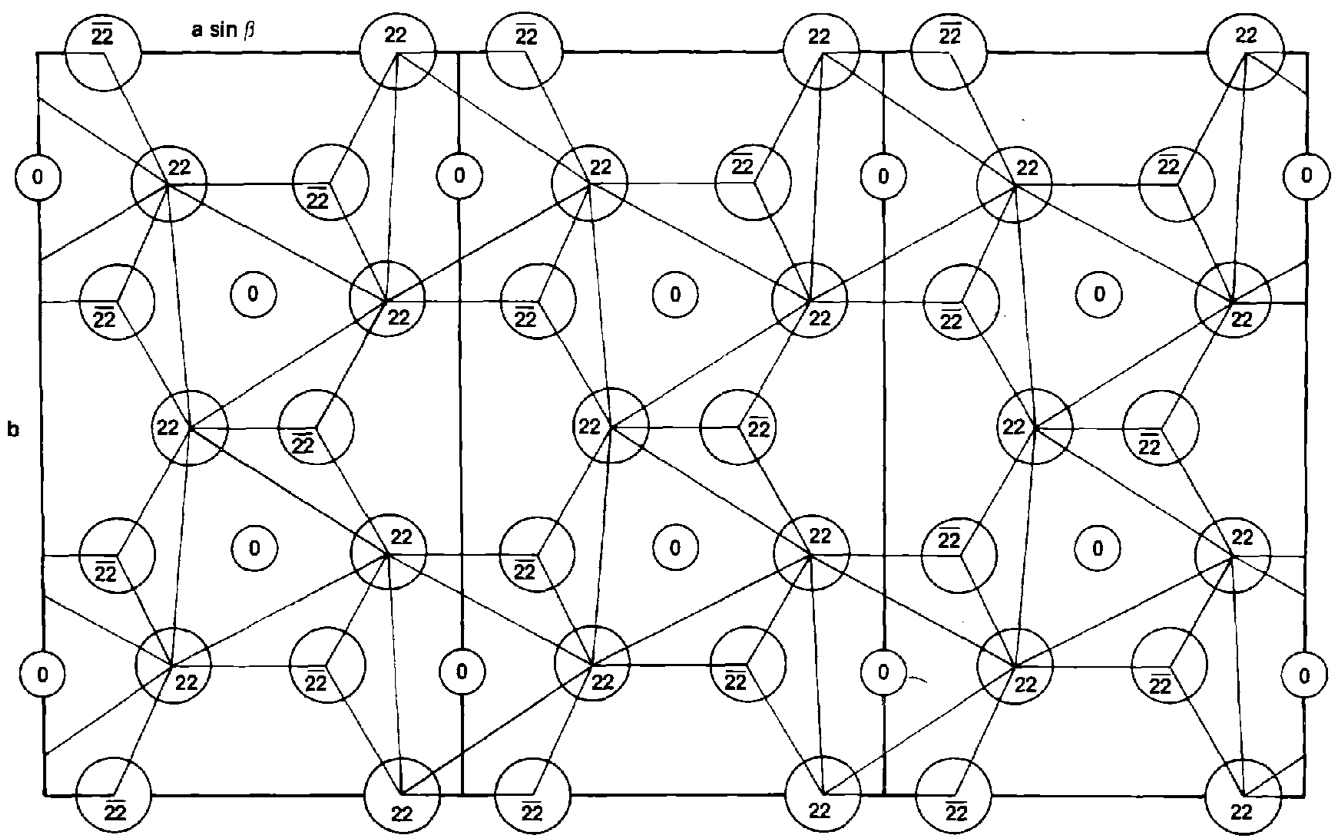

FIGURE 2. - One layer of $AlCl_3$, projected on the (001) plane, showing pseudohexagonal symmetry.

framework of AlF_6 octahedra, with shared corners, and is much more stable. It is rhombohedral, space group R32 (No. 155), with atoms in the following positions:

Al : (2c) xxx; $\bar{x}\bar{x}\bar{x}$; x=0.237

F(1) : (3d) $0x\bar{x}$; $\bar{x}0x$; $x\bar{x}0$; x=0.430

F(2) : (3e) $\frac{1}{2}x\bar{x}$; $\bar{x}\frac{1}{2}x$; $x\bar{x}\frac{1}{2}$; x=0.070

The corresponding hexagonal coordinates are--

Al : (6c) 00z; $00\bar{z}$; Rh; z=0.237

F(1) : (9d) x00; $0\bar{x}0$; $\bar{x}\bar{x}0$; Rh; x=0.430

F(2) : (9e) $x0\frac{1}{2}$; $0x\frac{1}{2}$; $\bar{x}\bar{x}\frac{1}{2}$; Rh; x=0.570

The structure, as shown in figures 3 and 4, is a deformed version of the simple cubic ReO_3 structure, with a slight expansion along one [111] axis. It is a defect cubic close-packed arrangement of F^- ions, with one-fourth of the sites vacant. All the available octahedral sites are occupied by Al^{3+} ions. The octahedra share all six corners with adjacent octahedra, forming a three-dimensional framework structure. The octahedra are distorted, with three F^- ions at 1.707 Å and three at 1.889 Å from the central Al^{3+} ion. The 12 edges of the octahedra are formed by F^- ions 2.537 Å apart. The F-F distances are somewhat less than the sum of the radii, 2.72 Å, and are most likely an indication of considerable polarization of the F^- ion. The stability of AlF_3, as compared with $AlCl_3$, is obviously a consequence of the stable octahedral coordination and the three-dimensional linkage.

CRYOLITE, Na_3AlF_6

Cryolite, Na_3AlF_6, is monoclinic, space group P2/n (No. 14); this places the unit

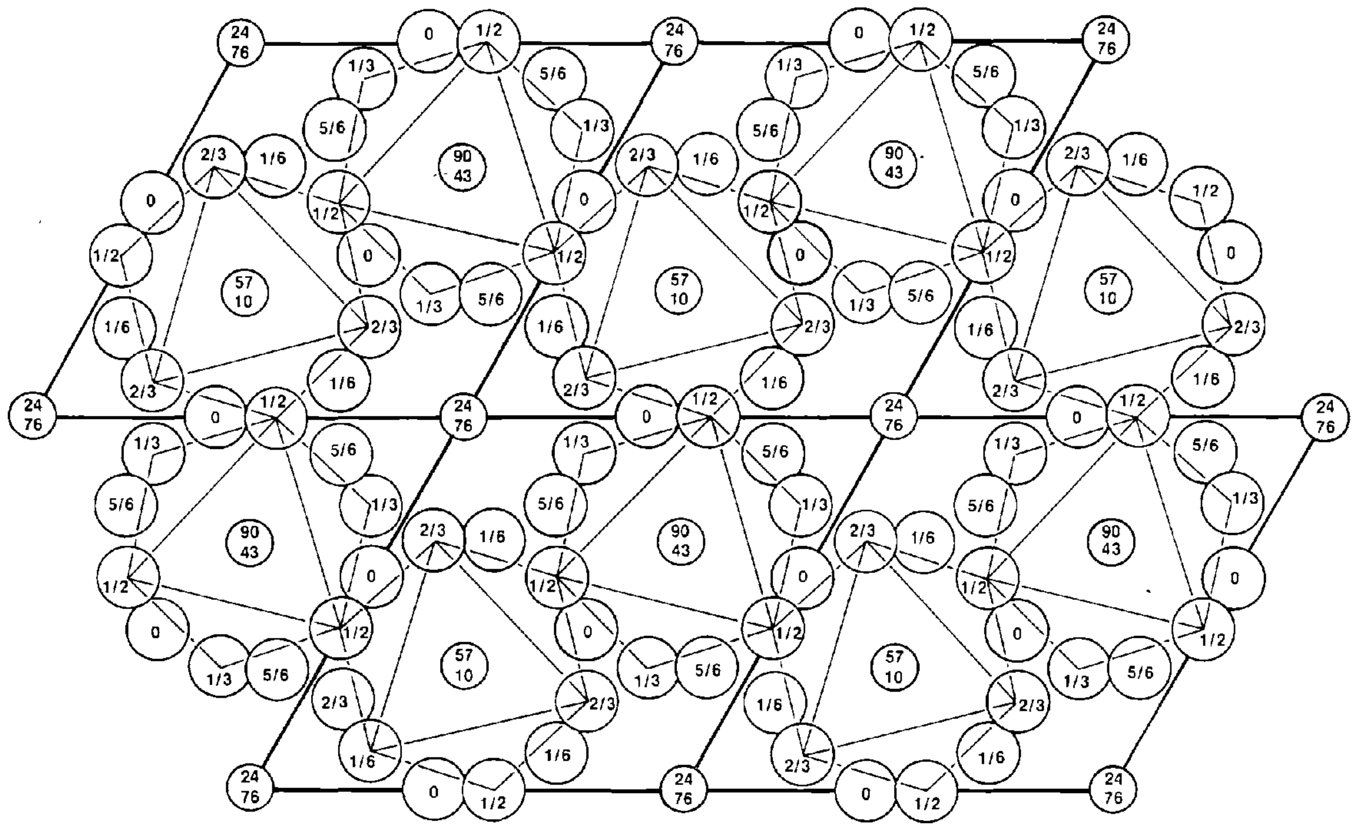

FIGURE 3. - The structure of hexagonal AlF_3, projected on the (0001) plane. Small atoms are Al; large atoms are F.

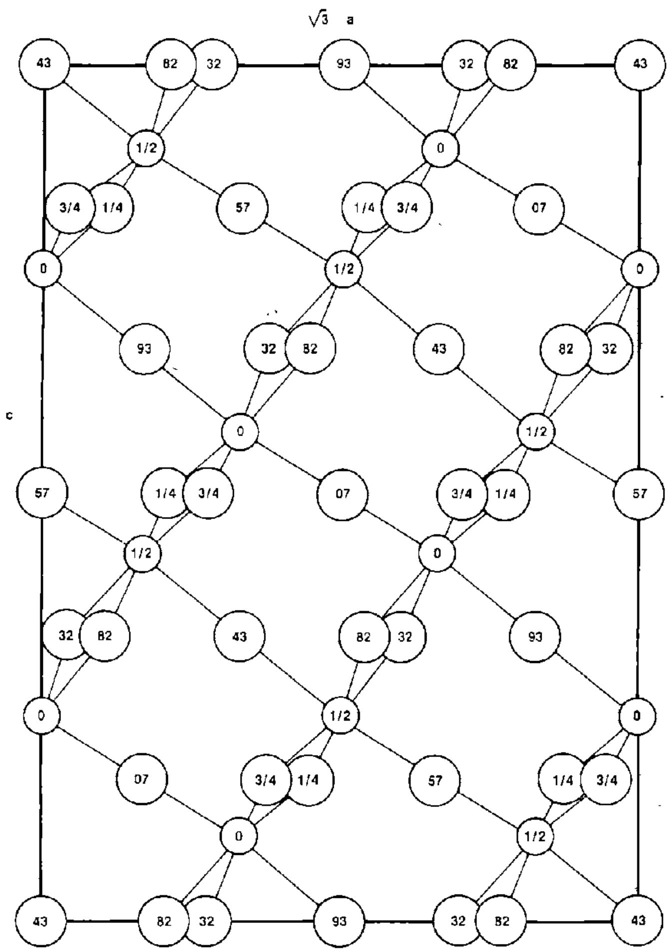

FIGURE 4. - The structure of hexagonal AlF_3, projected on the $(11\bar{2}0)$ plane.

cell in an alternate setting of space group $P2_1/c$. The atoms are located at--

Al : (2a) $000;\ \frac{111}{222}$

Na(1) : (2b) $00\frac{1}{2};\ \frac{11}{22}0$

Na(2) : (4c) $\pm\left(xyz;\ \frac{1}{2}+x,\frac{1}{2}-y,\frac{1}{2}+z\right);$

x=0.50; y=0.945; z=0.24

F(1) : (4c) x=0.065; y=0.06; z=0.22

F(2) : (4c) x=0.71; y=0.16; z=0.03

F(3) : (4c) x=0.15; y=0.28; z=0.94

The structure, shown in figure 5, is a pseudocubic close-packed arrangement of F^- ions with one-fourth of the sites vacant. The octahedral sites are occupied by Al^{3+} and one-third of the Na^+ ions in an ordered, alternating arrangement, forming a framework structure with all octahedra sharing corners with adjacent octahedra. The octahedral framework of the cryolite structure is a distortion of the AlF_3 structure, with half the sites occupied by Na^+ ions, rather than Al^{3+} ions. The remaining Na^+ are in interstitial sites with a highly distorted octahedral coordination. Interionic distances in the cryolite structure are listed in table 3. The Al-F and Na-F distances are comparable to those in AlF_3 and NaF, respectively, and the F-F distances in the AlF_6 octahedron are slightly less than the sum of the F^- radii, indicating a strongly bonded structure. As is indicated later, the high-temperature stability of cryolite is comparable with those of NaF and AlF_3.

TABLE 3. - Interionic distances in the cryolite structure

Ions	Number of ions	Interionic distance, Å
Al-F, octahedron.....	2	1.783
	4	1.834
NaF, octahedron......	2	2.332
	4	2.237
Na-F, interstitial....	1	2.211
	2	2.338
	2	2.466
	1	2.778
F-F, AlF_6 octahedron.	2	2.500
	2	2.552
	2	2.562
	4	2.594
	2	2.617
F-F, NaF octahedron..	2	2.985
	2	2.988
	2	3.206
	2	3.242
	2	3.333
	2	3.449

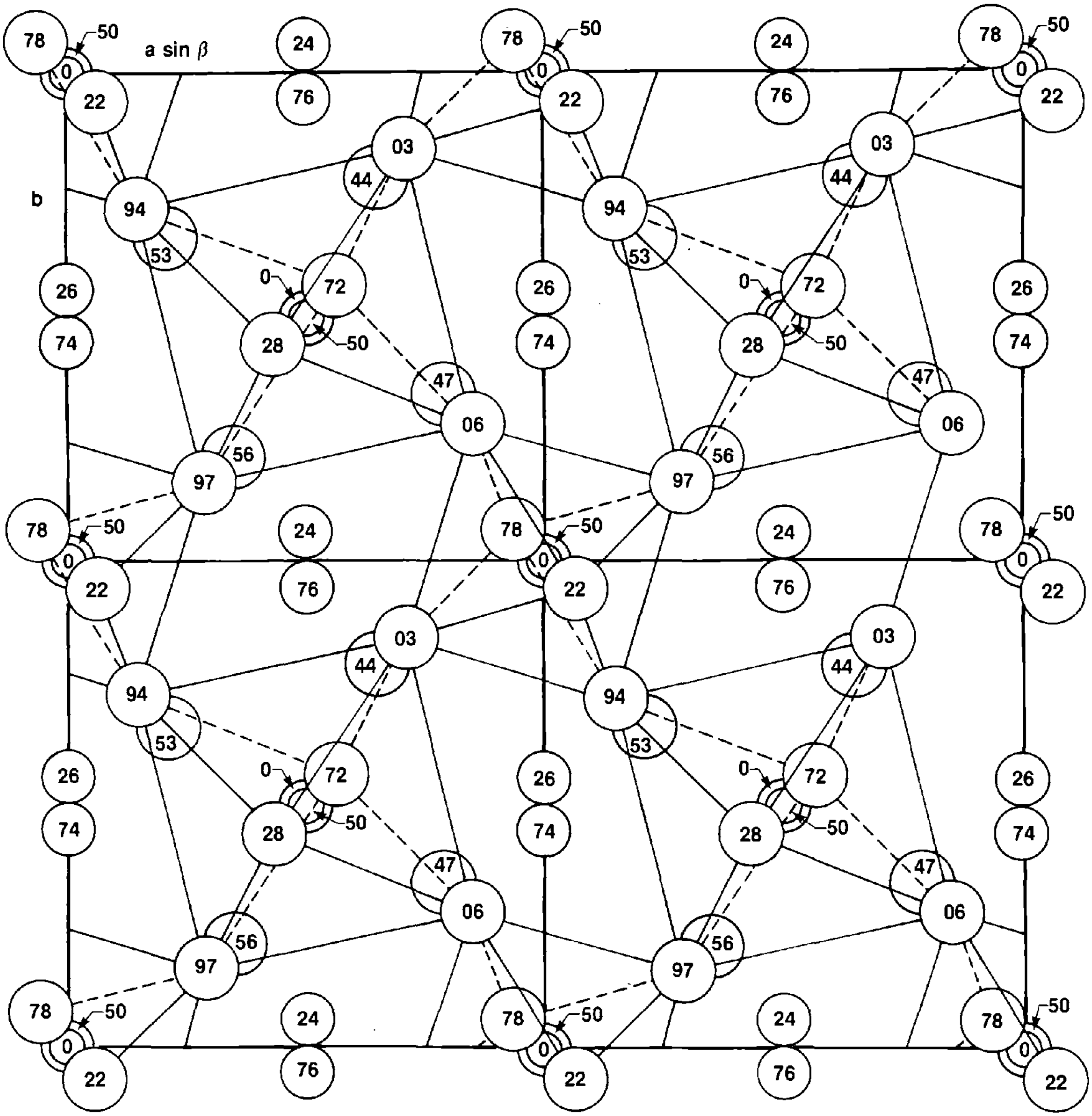

FIGURE 5. - The structure of cryolite, Na_3AlF_6, projected on the (001) plane. Small atoms are Al, intermediate-sized atoms are Na, large atoms are F.

POTASSIUM CRYOLITE, K_3AlF_6

The exact structure of K_3AlF_6, commonly referred to as K-cryolite, has not been determined. It was originally described as cubic (6) and is still indexed as such in the incomplete data in the Powder Diffraction Files. (See table 1.) Later work showed, however, that it is tetragonal, with parameters near those listed in table 1. If it is assumed that the structure is a tetragonal distortion of the structure originally assigned to it, the correct space group is I4/mmm (No. 139), with atoms located at--

$$Al : (2a)\ 000;\ \tfrac{1}{2}\tfrac{1}{2}\tfrac{1}{2}$$

$$K(1) : (2d)\ 00\tfrac{1}{2};\ \tfrac{1}{2}\tfrac{1}{2}0$$

$$K(2) : (4d)\ 0\tfrac{1}{2}\tfrac{1}{4};\ \tfrac{1}{2}0\tfrac{1}{4};\ \tfrac{1}{2}0\tfrac{3}{4};\ 0\tfrac{1}{2}\tfrac{3}{4}$$

$$F(1) : (4e)\ \pm\left(00z;\ \tfrac{1}{2},\tfrac{1}{2},\tfrac{1}{2}+z\right);\ z\approx 0.20$$

$$F(2) : (8h)\ \pm\left(xx0;\ x\bar{x}0;\ \tfrac{1}{2}+x,\tfrac{1}{2}+x,\tfrac{1}{2};\ \tfrac{1}{2}+x,\tfrac{1}{2}-x,\tfrac{1}{2}\right);\ x\approx 0.20$$

The structure, based on these data, is shown in figure 6. Though the lattice parameters and symmetry are different from those of cryolite, Na_3AlF_6, the structure of Na_3AlF_6 is quite similar. It consists of a framework of alternating AlF_6 and KF_6 octahedra, with the remaining K^+ ions in interstitial sites. Unlike the Na^+ ion, which occupies the highly distorted interstitial octahedral site, the larger K^+ props the structure open and occupies a distorted cubo-octahedral position. The interionic distances are listed in table 4. The Al-F distances are significantly less than in cryolite (table 3), the K-F distances are less than in KF (table 2), and the F-F distances in the AlF_6 octahedra are greater than in cryolite (table 3). This indicates the structural data are not very accurate. The correct space group is probably P4/mnc (No. 128), and the structure is a slight distortion of that shown in figure 6. This alternative structure is shown in figure 7. The differences between the structures are very slight and not significant in terms of the stability of the phase; it is to be expected that high-temperature properties of K_3AlF_6 will be comparable to those of Na_3AlF_6, as proves to be the case.

TABLE 4. - Interionic distances in K_3AlF_6

Ions	Number of ions	Interionic distance, Å
Al-F, octahedron.....	4	1.681
	2	1.694
K-F, octahedron......	4	2.540
	2	2.522
K-F, interstitial....	4	3.002
	8	3.012
F-F, AlF_6 octahedron.	4	2.378
	8	2.386
F-F, KF_6 octahedron..	4	3.566
	8	3.580

ELPASOLITE, K_2NaAlF_6

The structure of elpasolite, as originally described (38), was placed in space group Pa3 (No. 205), with atoms at--

Al: (4a) $000;\ \frac{1}{2}0\frac{1}{2};\ \frac{1}{2}\frac{1}{2}0;\ 0\frac{1}{2}\frac{1}{2}$

Na: (4b) $\frac{1}{2}\frac{1}{2}\frac{1}{2};\ 0\frac{1}{2}0;\ 00\frac{1}{2};\ \frac{1}{2}00$

K: (8c) $\pm\left(xxx,\ \frac{1}{2}+x,\frac{1}{2}-x,\bar{x};\ \bar{x},\frac{1}{2}+x,\frac{1}{2}-x;\ \frac{1}{2}-x,\bar{x},\frac{1}{2}+x\right);\ x=0.25$

F: (24d) $\pm\Big(xyz;\ zxy;\ yzx;\ \frac{1}{2}+x,\frac{1}{2}-y,\bar{z};\ \frac{1}{2}+z,\frac{1}{2}-x,\bar{y};$

$\frac{1}{2}+y,\frac{1}{2}-z,\bar{x};\ \bar{x},\frac{1}{2}+y,\frac{1}{2}-z;\ \bar{z},\frac{1}{2}+x,\frac{1}{2}-y;$

$\bar{y},\frac{1}{2}+z,\frac{1}{2}-x;\ \frac{1}{2}-x,\bar{y},\frac{1}{2}+z;\ \frac{1}{2}-z,\bar{x},\frac{1}{2}+y;\ \frac{1}{2}-y,\bar{z},\frac{1}{2}+x\Big);$

$x=0.22;\ y=0.03;\ z=0.01$

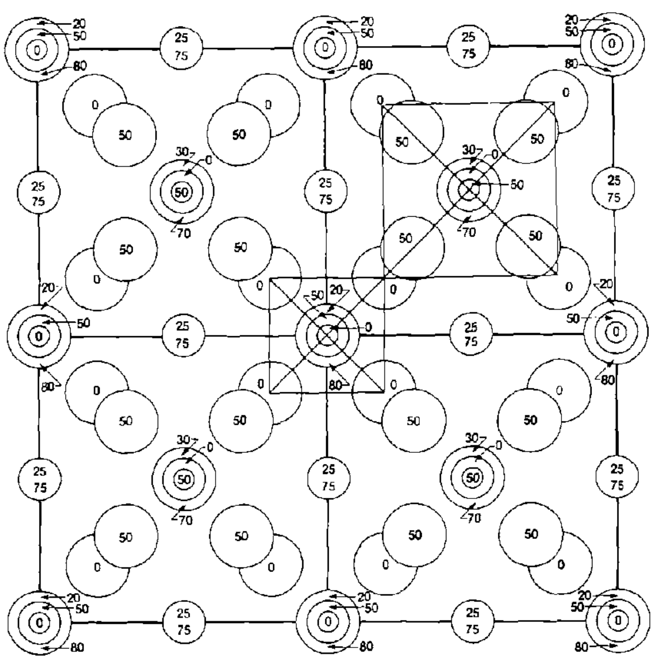

FIGURE 6. - The structure of K-cryolite, K_3AlF_6, projected on the (001) plane. Space group is assumed to be I4/mmm. Small atoms are Al; intermediate-sized atoms are K; large atoms are F.

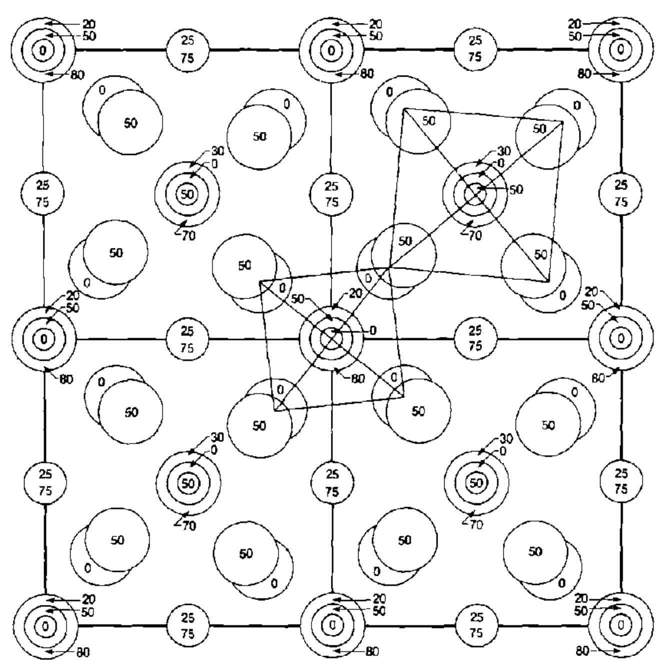

FIGURE 7. - An alternative structure for K-cryolite, assuming space group P4/mnc.

The structure thus defined is shown in figure 8. As is the case with cryolite, the structure consists of a framework of alternating AlF_6 and NaF_6 octahedra linked by shared corners in all three dimensions. The K^+ ions are all located in interstitial cubo-octahedral sites, as is the case with K_3AlF_6. The higher symmetry is a consequence of the ordering of Na^+ and K^+ ions in octahedral and cubo-octahedral sites, respectively. The similarity between the elpasolite structure and the structures of Na_3AlF_6 and K_3AlF_6 (figs. 5-7) may be seen in the tetragonal subcell indicated by dot-dash lines in figure 8. The interionic distances are listed in table 5. The metal-fluoride distances are comparable to those in cryolite and those in AlF_3, NaF, and KF, so it is reasonable to expect the high-temperature properties to be comparable with those phases, as proves to be the case.

There is some question in the literature about the details of the structure of elpasolite. Though Menzer (38) placed the structure in space group Pa3, several other authors (21, 59, 62) contend that X-ray and paramagnetic resonance data show the correct space group to be Fm3m. The atomic coordinates listed above show that the differences between the two choices are very slight. If the x, y, and z coordinates of the fluoride ion were shifted from 0.22, 0.03, and 0.01 to 0.25, 0.00, and 0.00, respectively, the symmetry would be changed from Pa3 to Fm3m, so the differences are insignificant.

TABLE 5. - Interionic distances in elpasolite

Ions	Number of ions	Interionic distance, Å
Al-F, octahedron.....	6	1.805
NaF, octahedron......	6	2.289
K-F, interstitial....	3	2.656
	3	2.777
	3	3.005
	3	3.113
F-F, AlF_6 octahedron.	6	2.306
	6	2.778
F-F, NaF_6 octahedron.	6	3.127
	6	3.343

CHIOLITE, $Na_5Al_3F_{14}$

Chiolite is tetragonal, space group P4/mnc (No. 128), with atoms located at--

Al (1): (2a) $000;\ \frac{1}{2}\frac{1}{2}\frac{1}{2}$

Al (2): (4c) $0\frac{1}{2}0;\ \frac{1}{2}00;\ 0\frac{1}{2}\frac{1}{2};\ \frac{1}{2}0\frac{1}{2}$

Na (1): (2b) $00\frac{1}{2};\ \frac{1}{2}\frac{1}{2}0$

Na (2): (8g) $\pm\left(x,\frac{1}{2}+x,\frac{1}{4};\ \frac{1}{2}+x,\bar{x},\frac{1}{4};\ \frac{1}{2}-x,x,\frac{1}{4};\ x,\frac{1}{2}+x,\frac{3}{4}\right)$; x=0.275

F (1): (4e) $\pm\left(00z;\ \frac{1}{2},\frac{1}{2},\frac{1}{2}+z\right)$; z=0.185

F (2): (8h) $\pm\left(xy0;\ \frac{1}{2}+x,\frac{1}{2}-x,\frac{1}{2};\ \bar{y}x0;\ \frac{1}{2}+y,\frac{1}{2}+x,\frac{1}{2}\right)$; x=0.07; y=0.25

$$F\ (3):\ (16i)\ \pm \left(xyz;\ \bar{x}\bar{y}z;\ \tfrac{1}{2}+x, \tfrac{1}{2}-y, \tfrac{1}{2}+z;\ \tfrac{1}{2}-x, \tfrac{1}{2}+y, \tfrac{1}{2}+z; \right.$$

$$\left. \bar{y}xz;\ y\bar{x}z;\ \tfrac{1}{2}+y, \tfrac{1}{2}+x;\ \tfrac{1}{2}+z;\ \tfrac{1}{2}-y, \tfrac{1}{2}-x, \tfrac{1}{2}+z \right);$$

$$x=0.21;\ y=0.535;\ z=0.12$$

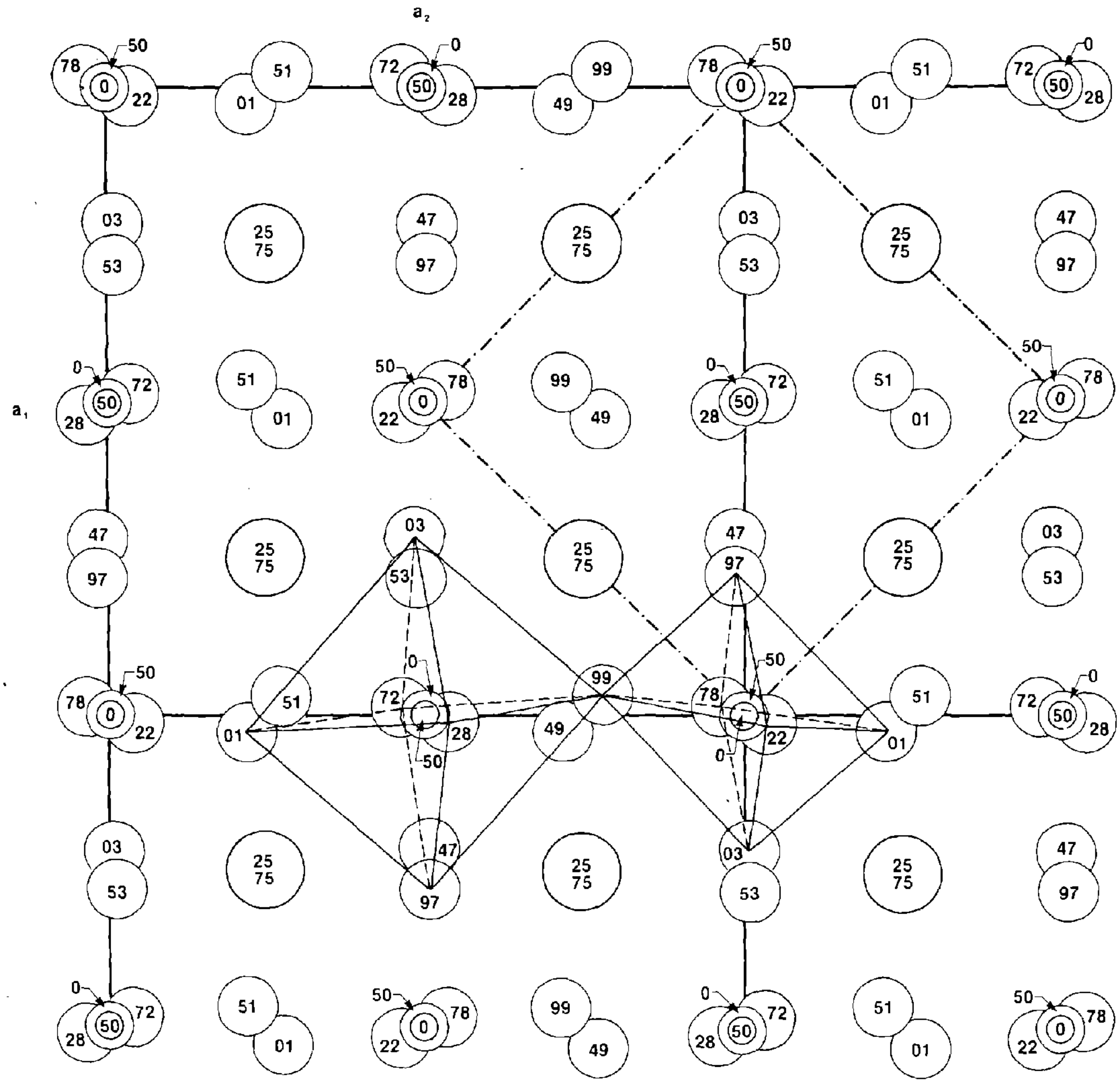

FIGURE 8. - The structure of elpasolite, K_2NaAlF_6, assuming space group Pa3. In order of increasing size, the atoms are Al, Na, F, and K.

One of the complex layers making up the structure is shown in figure 9. The layer is composed of two kinds of AlF_6 octahedra; half the octahedra share four corners, and the other half share two corners with adjacent octahedra. One-third of the Na^+ ions are located within the layer, surrounded by eight equidistant F^- ions. The remaining Na^+ ions are located between the layers, as shown in figure 10, surrounded by F^- ions in a highly distorted octahedral arrangement. There is no octahedral linkage between layers; the Na-F bonds serve to hold the

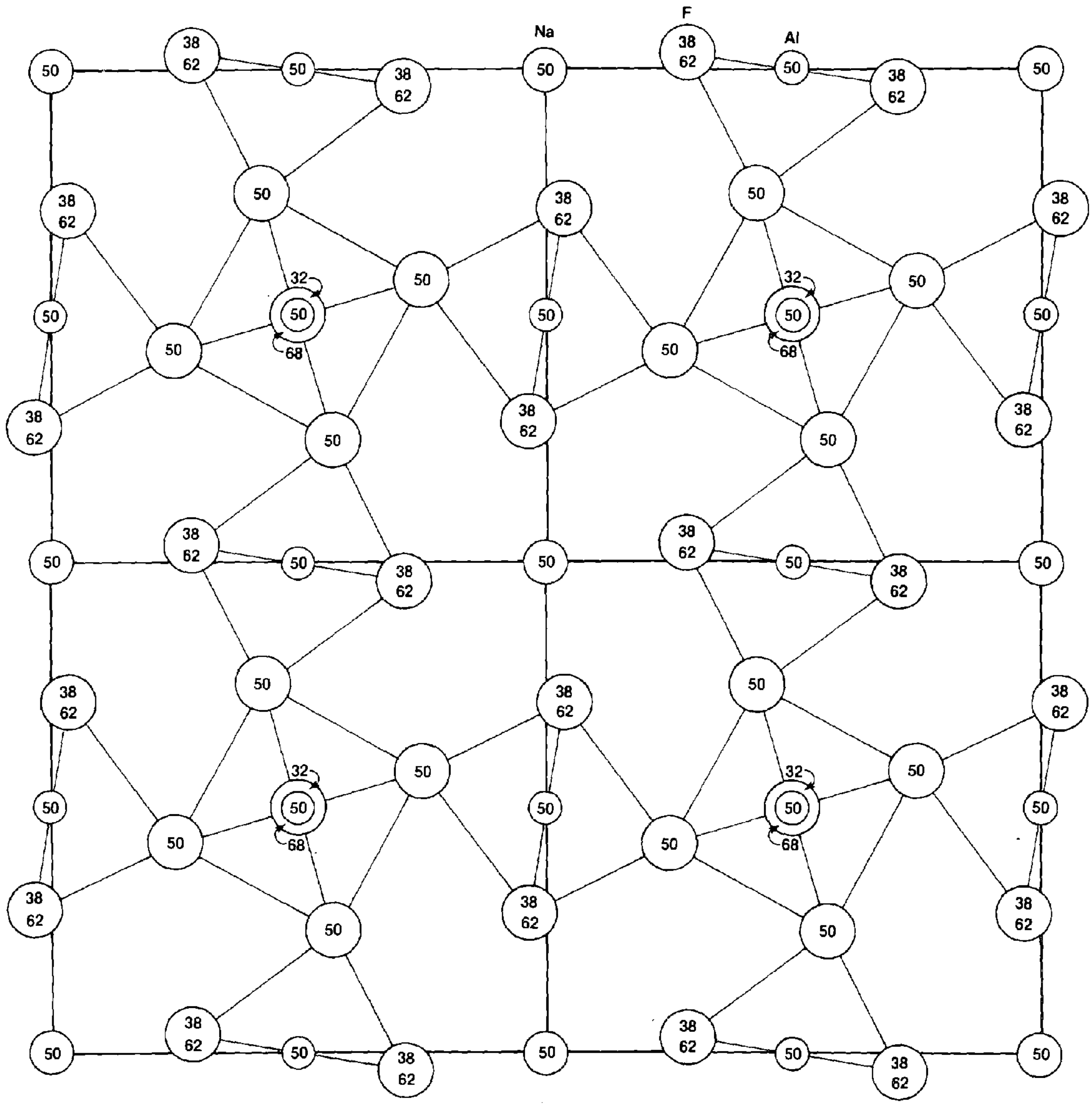

FIGURE 9. - The structure of one layer of chiolite, $Na_5Al_3F_{14}$, projected on the (001) plane.

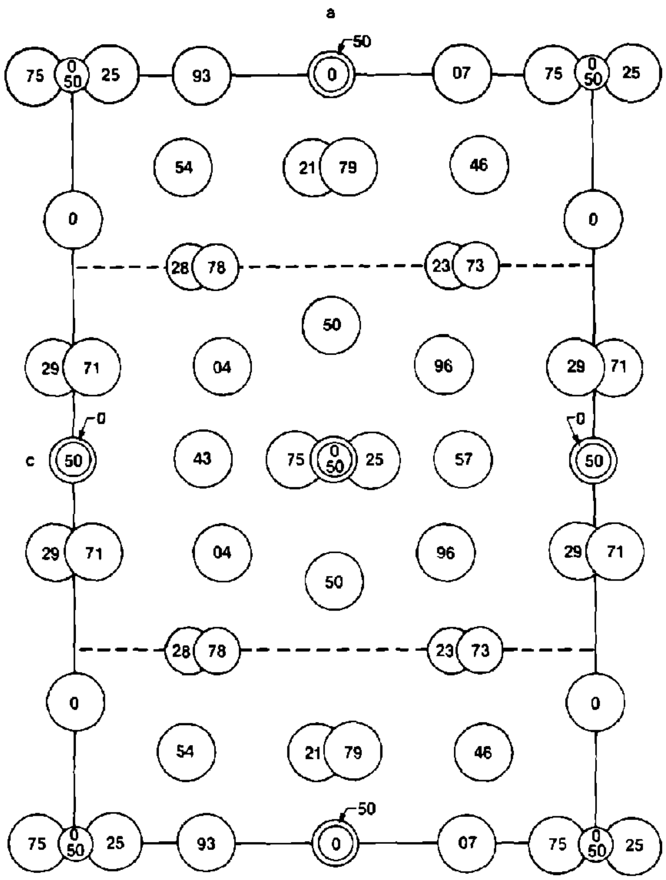

FIGURE 10. - The structure of chiolite, projected on the (100) plane.

TABLE 6. - Interionic distances in chiolite

Ions	Number of ions	Interionic distance, Å
Al(1)-F, octahedron..	6	1.821
Al(2)-F, octahedron..	2	1.821
	4	1.946
Na(1)-F, intralayer..	8	2.399
Na(2)-F, interlayer..	2	2.207
	2	2.273
	1	2.582
	1	2.611
F-F, Al(1)-F octahedron..........	12	2.575
F-F, Al(2)-F octahedron..........	2	2.496
	4	2.553
	4	2.773
	2	2.987

layers together. The interionic distances, listed in table 6, are comparable to those in AlF_3, cryolite, and NaF, indicating stabilities comparable with those phases.

$KAlF_4$ AND $NaAlF_4$

The potassium and sodium tetrafluoroaluminates are isostructural, space group P4/mmm (No. 123), with atoms located at--

Na or K: (1a) 000

Al: (1d) $\frac{1}{2}\frac{1}{2}\frac{1}{2}$

F(1): (2e) $0\frac{1}{2}\frac{1}{2}$; $\frac{1}{2}0\frac{1}{2}$

F(2): (2h) $\frac{1}{2}\frac{1}{2}z$; $\frac{1}{2}\frac{1}{2}\bar{z}$; $z \approx 0.21$

The structure, shown in figure 11, consists of layers of AlF_6 octahedra, each sharing four corners with adjacent octahedra. All the Na^+ or K^+ ions are located between the layers, surrounded by eight F^- ions on the corners of a tetragonal prism. The interionic distances are listed in tables 7 and 8. The Al-F and F-F distances are comparable with those in AlF_3 and cryolite, but the Na-F and K-F distances are significantly greater than in the corresponding alkali fluorides and hexafluorides (tables 2-5). The K-F distance in $KAlF_4$ is 5.5 pct greater than in KF, leading to weak bonding between the layers, accounting for the low melting point (5, 44). The Na-F distance in $NaAlF_4$ is 18 pct greater than in NaF; this is in accord with the observation that $NaAlF_4$ is unstable with respect to chiolite, $Na_5Al_3F_{14}$, and has probably been formed only as a metastable phase via vapor deposition (5, 24, 37), although it has been reported as a stable phase (17).

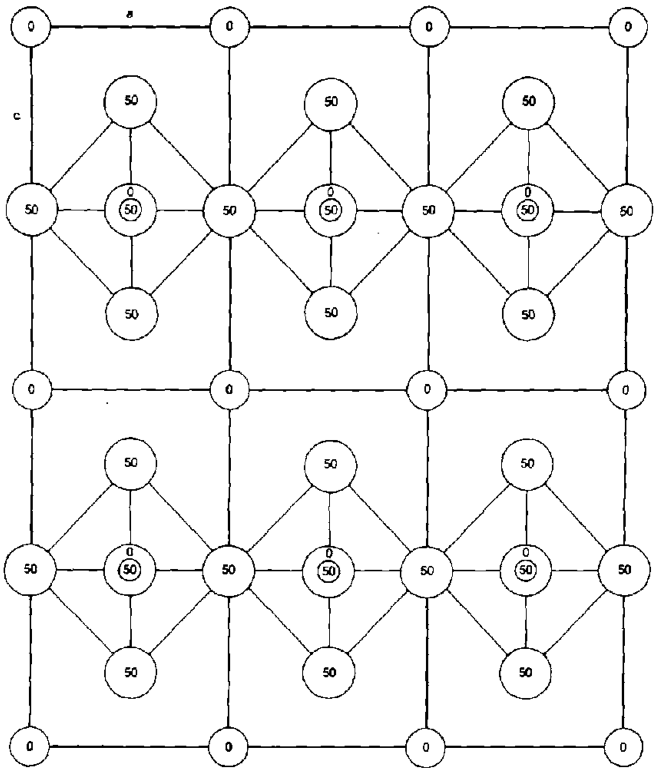

FIGURE 11. - The structures of $NaAlF_4$ and $KAlF_4$. Alkali ions are shown as intermediate-sized circles; small atoms are Al; large atoms are F.

$NaAlCl_4$ AND $KAlCl_4$

The structure of $NaAlCl_4$ has been assigned to the orthorhombic space group $P2_12_12_1$ (No. 18), with atoms located in the general positions--

$$(4a):\quad xyz;\ \frac{1}{2}-x,\bar{y},z;\ \frac{1}{2}+x,\frac{1}{2}-y,\bar{z};\ \bar{x},\frac{1}{2}+y,\frac{1}{2}-z$$

with the following coordinates:

Atom	x	y	x
Na	0.128	0.207	0.677
Al	.039	.485	.204
Cl(1)	.031	.490	.552
Cl(2)	.148	.316	.105
Cl(3)	.348	.024	.923
Cl(4)	.379	.336	.577

The structure, shown in figure 12, is made up of independent $AlCl_4$ tetrahedra held together by Na^+ ions in the interstitial positions. The interionic distances are listed in table 9. The Al-Cl distances are somewhat less than the

TABLE 7. - Interionic distances in $KAlF_4$

Ions	Number of ions	Interionic distance, Å
Al-F................	4	1.775
	2	1.783
K-F.................	8	2.822
F-F, octahedral......	8	2.510
	4	2.514
F-F, interlayer......	1	2.578

TABLE 8. - Interionic distances in $NaAlF_4$

Ions	Number of ions	Interionic distance, Å
Al-F................	4	1.740
	2	1.824
Na-F................	8	2.793
F-F, octahedral......	8	2.461
	4	2.521
F-F, interlayer......	1	2.642

octahedral distances in $AlCl_3$, indicating a more stable coordination. Only two of the Na-Cl distances, however, are near the value of 2.802 Å in the NaCl structure (table 2), explaining the low melting point for the phase.

X-ray diffraction analysis of the structure of $KAlCl_4$ has not been done. The unit cell is monoclinic, rather than orthorhombic, but Raman spectroscopy (53) indicates an independent tetrahedral structure, probably a distortion of the $NaAlCl_4$ structure.

SUMMARY OF CRYSTAL CHEMISTRY

The crystal structures of phases in the system $NaCl$-KCl-$AlCl_3$-NaF-KF-AlF_3 are essentially of two groups: (1) those in which all the metal-halide distances are such that the interionic potential energy is near the minimum and the linkage of

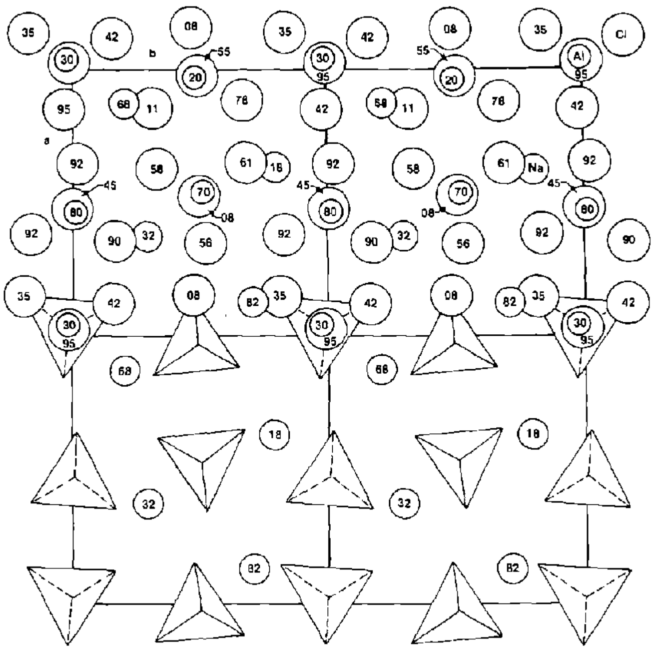

FIGURE 12. - The structure of $NaAlCl_4$, projected on the (001) plane. Small atoms are Al; intermediate-sized atoms are Na; large atoms are F. AlF_4^- tetrahedra are shown in the lower unit cells.

TABLE 9. - Interionic distances in $NaAlCl_4$

Ions[1]	Interionic distance, Å
Al-Cl, tetrahedron...........	2.113
	2.121
	2.132
	2.163
Na-Cl, interstitial..........	2.793
	2.877
	2.964
	3.054
	3.081
	3.290
Cl-Cl, tetrahedral edges.....	3.388
	3.468
	3.486
	3.494
	3.509
	3.543

[1] 1 ion in all instances.

octahedral units, through shared faces or corners, produces a three-dimensional network, and (2) those in which geometric and electrostatic conditions are such that neither of those two conditions can be met, so that some ions are in sites too large or the development of a three-dimensional network is not possible. The former group, consisting of the alkali halides, AlF_3, cryolite, K-cryolite, elpasolite, and chiolite, have relatively high melting points and low vapor pressures. The latter group, consisting of $AlCl_3$ and the alkali tetrafluoroaluminates and tetrachloroaluminates, have relatively low melting points and high vapor pressures. The relationship between crystalline structure and the structure and properties of the liquid phase is not clear, but it is reasonable to expect a dependence on the ratios of the different ions, particularly as those ratios will affect the distribution of aluminum halide octahedral and tetrahedral species in the melt.

PHASE EQUILIBRIA

A large body of literature describing the melting characteristics of compositions within the system $NaCl$-KCl-$AlCl_3$-NaF-KF-AlF_3 exists, but it is by no means complete, nor is it entirely reliable. There are numerous disagreements as to melting temperatures and many contradictions as to the compositions of the crystalline phases. Following is a summary of the most important information now available.

MELTING POINTS AND TRANSITION TEMPERATURES

Alkali Halides

The chlorides and fluorides of sodium and potassium are remarkably similar, not only in structure, but also in terms of thermal properties. The melting points reported are 800° C (30) to 805° C (11) for NaCl; 722° C (47) to 774° C (11) for

KCl; 990° C (47) to 994.5° C (23) for NaF; and 850° C (47) to 858.4° C (23) for KF. Equilibrium vapor pressures for these phases are relatively low, and they show little tendency to react with atmospheric moisture to hydrolyze to the oxide and the acid. The high melting points and low vapor pressures are consequences of the intrinsic stability of the rock salt structure; the ions are in stable coordination and the polyhedral sharing results in a strongly bonded, isotropic structure.

Aluminum Halides

The aluminum halides are strikingly different in structure and properties. The unbonded layer structure (figs. 1-2) and the unstable octahedral coordination of $AlCl_3$ result in a very unstable phase. Melting points of 190.2° C (26) and 193.3° C (30) have been reported; these values were obtained from visual observation of crystallization in sealed glass tubes at pressures greater than 760 torr. At atmospheric pressure, $AlCl_3$ sublimes at 180.2° C, and the triple point for coexistence of solid, liquid, and vapor has been placed at 192.6° C and 1,715 torr (56). In the presence of atmospheric moisture, $AlCl_3$ hydrolyzes readily to form $Al(OH)_3$ and HCl, so it is necessary to conduct experimental work in a completely dry environment.

The three-dimensional octahedral framework and stable coordination of AlF_3 result in a much more stable phase. The melting point has been reported as 990° C in a sealed container (44), but this value cannot be correct because the phase sublimes at 1,265° C at 760 torr (50, 64); the triple point has not yet been determined. AlF_3 also hydrolyzes readily in the presence of atmospheric moiture to form $Al(OH)_3$ or Al_2O_3, depending on temperature, and HF.

Alkali Hexafluoroaluminates

Cryolite, Na_3AlF_6, undergoes a reversible transition from monoclinic to cubic symmetry at 561° C (35); melting temperatures between 1,000° C (36) and 1,009° C (10) have been reported. The relatively high melting point and low vapor pressures are consequences of the three-dimensional octahedral network formed by alternating AlF_6 and NaF_6 octahedra. K-cryolite, K_3AlF_6, which is structurally very similar to cryolite, also has a relatively high melting point, 985° C (44) to 986° C (36). Steward (59) reported K_3AlF_6 to be tetragonal, pseudocubic at 25° C, with the c/a ratio changing gradually to 300° C, at which temperature it is strictly cubic.

Elpasolite, which has been given the formula K_2NaAlF_6, has not been well studied. Only one value of the melting point, 932° C, has been reported (36), and no property measurements have been made. As indicated later in this report, the phase has a wide range of composition and is strictly cubic. It is to be expected, because of the chemical and structural similarity between elpasolite, cryolite, and K-cryolite, that the properties will be similar across the whole system Na_3AlF_6-K_3AlF_6.

Chiolite

Chiolite, $Na_5Al_3F_{14}$, melts incongruently at 741° C to cryolite and liquid containing 30 wt pct AlF_3 (13). The relatively high melting point is a result of the stable coordination of the Na^+ ion between the octahedral layers, but the structure is considerably less stable than that of cryolite.

Alkali Tetrafluoroaluminates

The phase $KAlF_4$ has definitely been established as a stable phase in the system KF-AlF_3. It melts incongruently at 574° C to form AlF_3 and a liquid only slightly richer in KF (44). The symmetry of $KAlF_4$ as a function of temperature is the subject of some disagreement. Grjotheim (17) reported the phase to be tetragonal at 25° C, with a transition to cubic symmetry at 327° C; Phillips (44) later reported it to be cubic at 25° C, with a transition to orthorhombic symmetry at approximately -15° C.

The sodium analog, $NaAlF_4$, which is isostructural with $KAlF_4$, is much less stable, and its existence as a stable phase at atmospheric pressure has been questioned. Grjotheim (17), for example, determined a melting point of 775° C, using thermal analyses. Foster (13), however, did a detailed study which indicated it did not form as a stable phase. Other work (10, 15, 24, 37, 39) indicates that it forms only as a metastable phase, most readily by vapor deposition, and is easily dissociated into $Na_5Al_3F_{14}$ and AlF_3. The layer structure of $KAlF_4$ and $NaAlF_4$ is such that, though the K^+ ion is large enough to maintain a stable structure, the Na^+ ion is not able to achieve a stable Na-F bond distance.

Alkali Tetrachloroaluminates

As indicated by the structural analysis (1), the Na-Cl bond distances are considerably greater than the sum of the ionic radii; the resultant instability of the phase is shown by the low melting point and high vapor pressures. The phase melts incongruently at 152° C (26) or 153° C (30) to NaCl and a liquid only slightly richer in $AlCl_3$. The $KAlCl_4$ phase has a higher melting point, 250° C (26, 55), also incongruent, forming KCl and a liquid only slightly richer in $AlCl_3$. The higher melting point of $KAlCl_4$ is a result of the larger radius of the K^+ ion, which is more stably coordinated with the Cl^- ions.

ALKALI HALIDE SYSTEMS[5]

The systems NaCl-KCl (11, 52) and NaF-KF (22), shown in figure 13, illustrate clearly the chemical differences between fluoride and chloride systems. NaCl and KCl form a complete solution series with a minimum liquidus temperature of 645° C at ~50 mol pct KCl; the solid solutions dissociate spinodally at lower temperatures, however. The consolute point is at ~500° C and ~35 mol pct KCl. Dissociation of the solid solutions proceeds at a rapid rate, with metastable equilibrium attained within an hour even at 25° C.

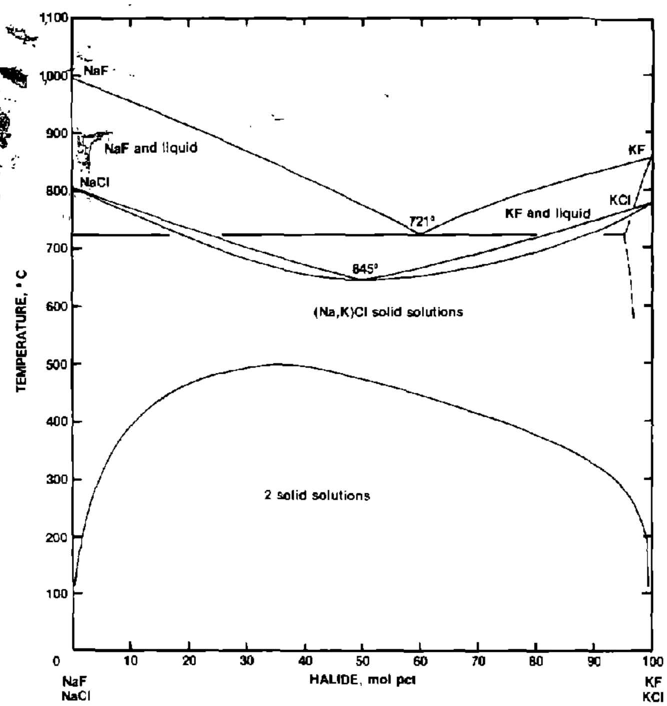

FIGURE 13. - The system NaF-KF, drawn from the data of reference 23, and the system NaCl-KCl, drawn from the data of references 11 and 52.

NaF and KF exhibit only slight solid solution on the KF-rich side, 5 mol pct NaF in KF; a eutectic is located at 721° C, 60 mol pct KF. The differences may be attributed to the fact that the F^- ion has a strong polarizing effect on the cations, making the structure much less adaptable to substitutional solid solution. The liquidus minimum, 645° C, in the system NaCl-KCl is just below the melting point of pure aluminum, 660° C, so a 50:50 mix of the two salts makes an ideal base composition for fluxing salts.

Interactions between NaF and the alkali chlorides, NaCl (18) and KCl (47), are very similar, as shown in figure 14. Both are simple eutectic systems, with no solid solubility; the eutectics and liquidus curves are quite close. The absence of substitutional solid solution between Cl^- and F^- is another indication of their intrinsic differences and the extent to which the F^- ion determines the properties of molten salts.

The remaining combination of mixed salts, NaCl-KF, is an unstable system; the phases react completely and irreversibly to form NaF and KCl (47).

---

[5]These and other diagrams in this report have been drawn from data of the original authors or redrawn from those in "Phase Diagrams for Ceramists" (31-33).

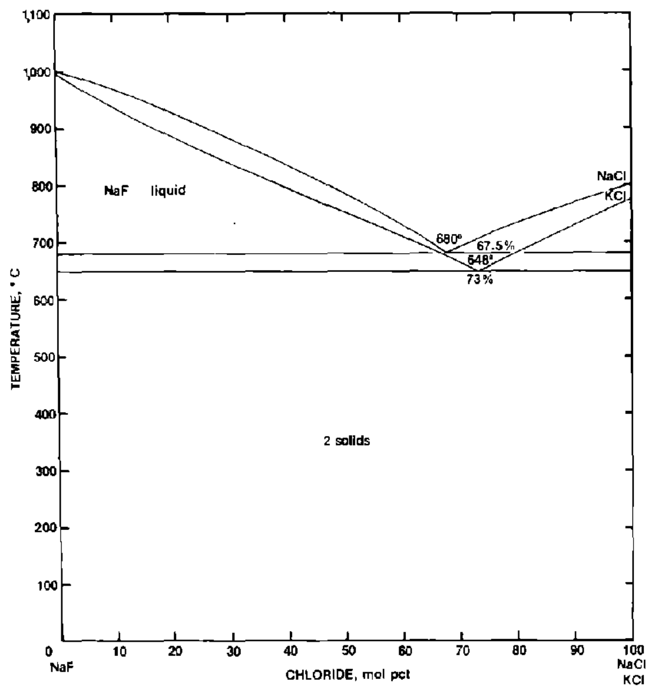

FIGURE 14. - The systems NaF-NaCl and NaF-KCl, drawn from the data of references 18 and 47.

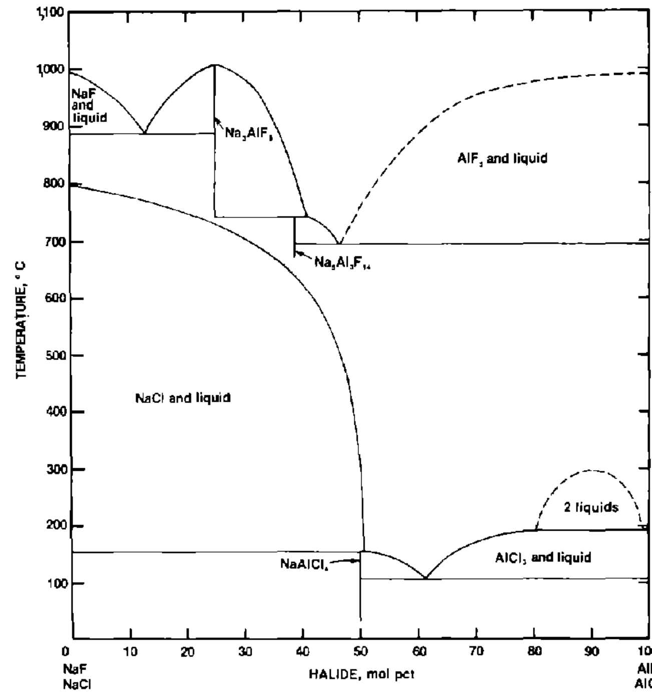

FIGURE 15. - The system NaF-AlF_3, drawn from the data of references 10 and 13, and the system NaCl-$AlCl_3$, drawn from the data of reference 30.

THE ALKALI HALOALUMINATES

The systems NaF-AlF_3 (10, 13) and NaCl-$AlCl_3$ (30), shown in figure 15, strikingly illustrate the fundamental difference between the effects of AlF_3 and $AlCl_3$ on the properties of salt systems. The structural stability of cryolite, Na_3AlF_6, with a melting point higher than NaF, is the dominant factor in the system NaF-AlF_3; the eutectic is at 888° C, ~13 mol pct AlF_3. Chiolite, $Na_5Al_3F_{14}$, melts incongruently to the more stable cryolite and a liquid with ~41 mol pct AlF_3; the eutectic between chiolite and AlF_3 is at 694° C, ~46 mol pct AlF_3. The liquidus curve for AlF_3 has not been determined; the high vapor pressures over AlF_3-rich liquids are such that sublimation of solid AlF_3 in the assemblage probably occurs at a composition near the eutectic at atmospheric pressure.

The unstable coordination of the Al^{3+} ion with Cl^- in $AlCl_3$ and the unstable coordination of the Na^+ ion with Cl^- in the $NaAlCl_4$ structure result in a very unstable system in NaCl-$AlCl_3$. The incongruent melting point of $NaAlCl_4$ is 152°-153° C, and the eutectic between $NaAlCl_4$ and $AlCl_3$ is at 107.2° C, 61.4 mol pct $AlCl_3$. The liquid miscibility gap, which has not been defined, extends from 191.3° C upward.

The systems KF-AlF_3 (44) and KCl-$AlCl_3$ (26, 40, 55), shown in figure 16, are quite similar to the sodium analogs. There is no potassium analog of chiolite, however, and $KAlF_4$ is a stable solid below 574° C. The greater stability of the K^+ ion in the structure of $KAlCl_4$ results in a melting point of 250° C, as compared with 152°-153° C for $NaAlCl_4$.

SODIUM HALIDE-CRYOLITE SYSTEMS

The NaF-rich portion (Na_3AlF_6) of the system NaF-AlF_3, shown previously in figure 15, as reported by Fuseya (14), and the system NaCl-Na_3AlF_6 (29) are shown for comparison in figure 17. Addition of NaCl to cryolite has a greater effect on liquidus temperatures than does addition of NaF. This is possibly a result of the competition between the Al^{3+} ion and the

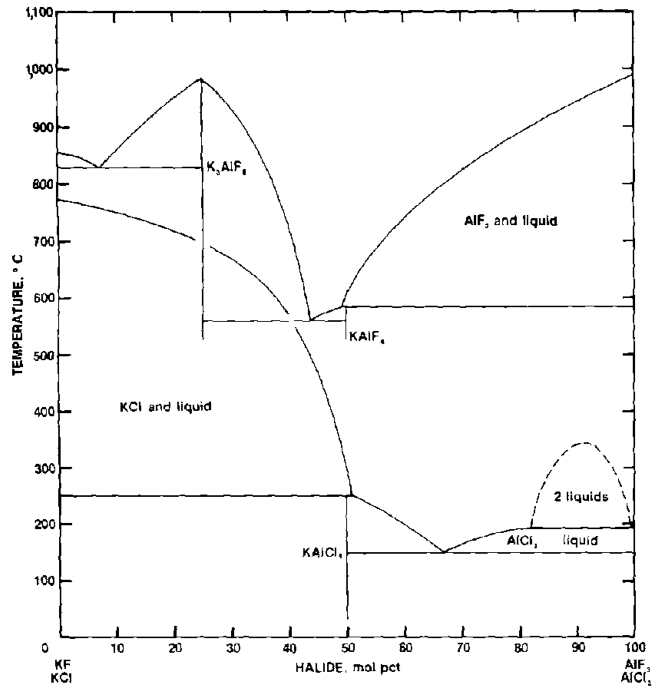

FIGURE 16. - The system KF-AlF_3, drawn from the data of references 26 and 44, and the system KCl-$AlCl_3$, drawn from the data of references 26, 40, and 55.

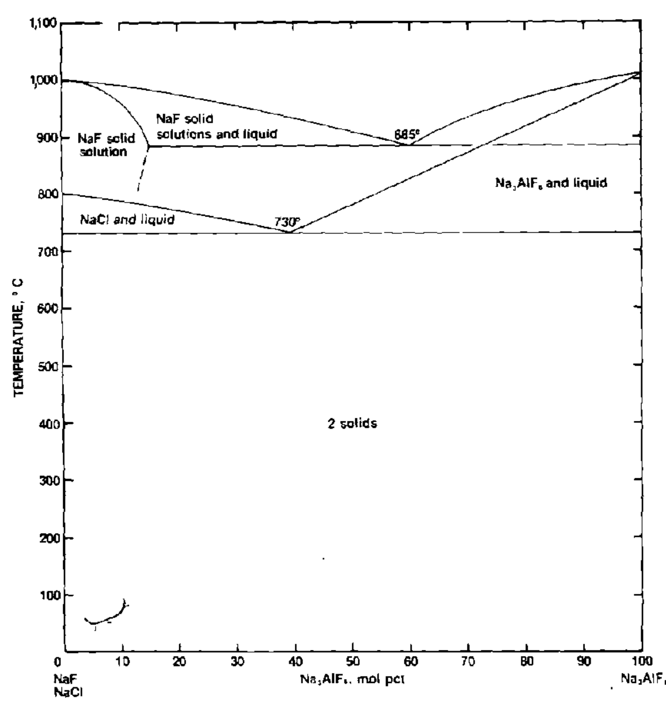

FIGURE 17. - The system NaF-Na_3AlF_6, drawn from the data of reference 14, and the system NaCl-Na_3AlF_6, drawn from the data of reference 29.

Na^+ for the F^- ions to form more stable octahedral units than can be formed with the Cl^- ions; in any case, the observation can be made that, in general, addition of chlorides to fluorides causes greater decreases in liquidus temperatures than does addition of one fluoride to another fluoride.

THE ALKALI CHLOROALUMINATES

The ternary system NaCl-KCl-$AlCl_3$ has not been well studied because of the experimental difficulties of working with very volatile, easily hydrolyzed samples. Barton (2) presented some preliminary data, but the high-$AlCl_3$ portion of the system was not covered and the completed study was apparently never published. Midorikawa (40-41) determined the peritectics and eutectics in the systems NaCl-$AlCl_3$ and KCl-$AlCl_3$ and liquidus isotherms in the low-melting portion of the ternary system. Figure 18 (top) shows a hypothetical interpretation of the system, based on the ternary data of Midorikawa (41); the bottom presents the complete system, based on binary data shown in figures 13, 15, and 16 and on the data of Barton (2). It must be emphasized that the diagram is hypothetical and that the equilibria in the high-$AlCl_3$ portion of the system would be valid only at pressures >760 torr. The assumption has been made that the immiscible liquids observed in the binary systems also exist as ternary liquids above 193° C and that $NaAlCl_4$ and $KAlCl_4$ form a complete solution series, at least just below solidus temperatures. This latter assumption is not in agreement with the work of Chikanov (9), who shows $NaAlCl_4$-$KAlCl_4$ as a simple binary system with a eutectic at 125° C, ~32 mol pct $KAlCl_4$.

MIXED ALKALI HALIDES

Compositions containing all four alkali halides--NaCl, KCl, NaF, and KF--do not melt in accordance with the characteristics of a quaternary system. This is because NaCl and KF are unstable in combination; they react completely and

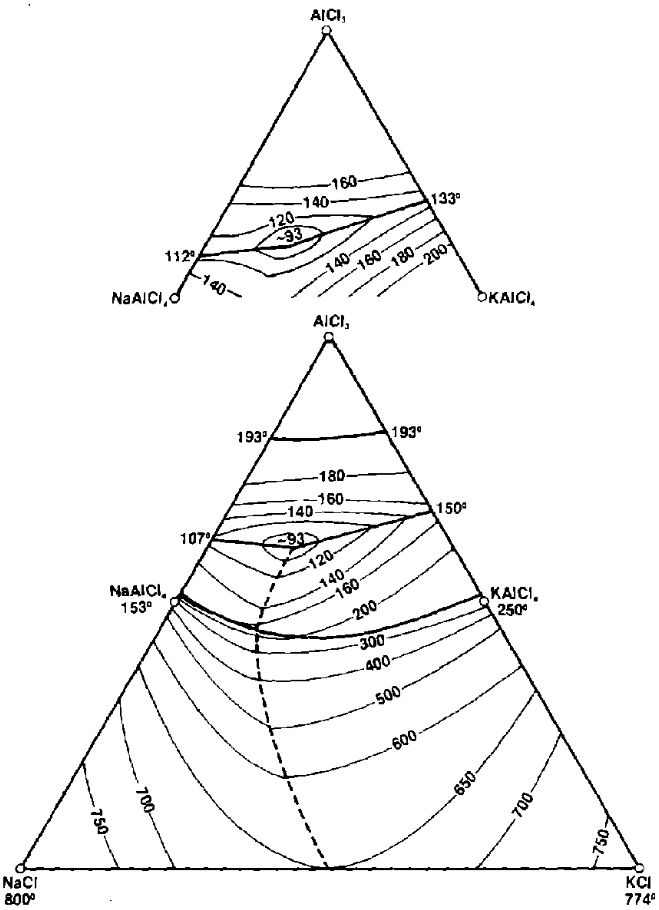

FIGURE 18. - The system $NaCl-KCl-AlCl_3$. Upper diagram redrawn from the data of reference 41. Lower diagram represents the system as inferred from the data of references 2, 19, and 41.

irreversibly at all temperatures to form NaF and KCl, the combination of small cations and anions and of large cations and anions lowering the lattice energies because of the more favorable radius ratios. Phase equilibria can be shown, therefore, as two ternary diagrams with only one common binary, in this case NaF-KCl. Liquidus temperatures for the ternaries were determined by Polyakov (47), as shown in figure 19, and by Ishaque (25), as shown in figure 20. Both authors indicated no solid solubility except for NaCl-KCl. Both diagrams show simple ternary eutectic relationships; the binary liquidus temperatures and eutectics are in reasonably good agreement with other authors' data.

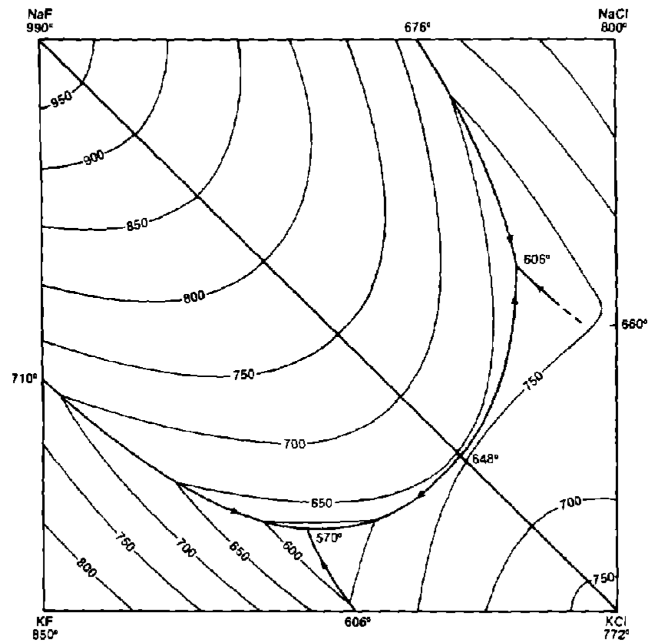

FIGURE 19. - The reciprocal system NaCl-KCl-NaF-KF, redrawn from the data of reference 47.

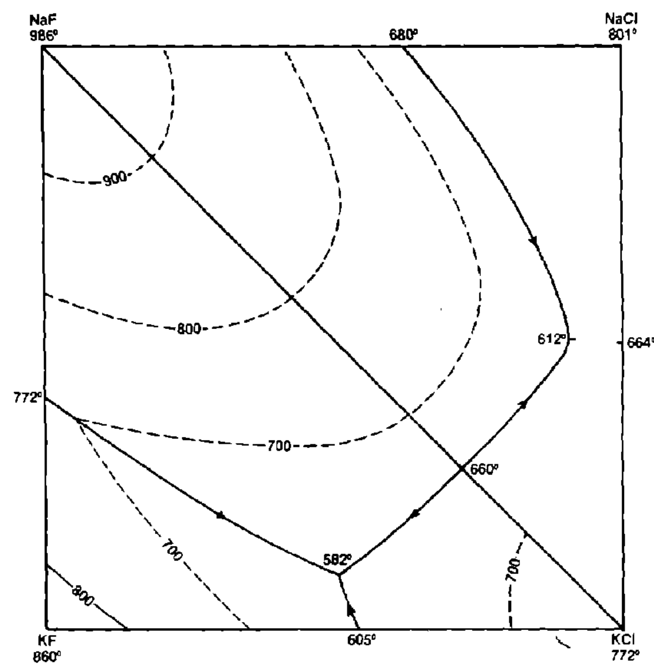

FIGURE 20. - The reciprocal system NaCl-KCl-NaF-KF, redrawn from the data of reference 25.

EQUILIBRIA IN THE SYSTEM $NaCl-KCl-AlCl_3-NaF-KF-AlF_3$

In addition to gaps in the information available about the system, there is considerable uncertainty about the compositions of the phases and their crystallization behavior. This is most obvious in the case of the binary relationships between Na_3AlF_6 and K_3AlF_6. In 1962 Bukhalova (7), in the first detailed study within the system, reported that a complete solid solution exists between Na_3AlF_6 and K_3AlF_6 and that phases in that binary exist in stable equilibria with NaCl-KCl solid solutions. Bukhalova's liquidus isotherms are shown in figure 21. No indication was given of the compositions of coexisting solid solutions, of the existence or nonexistence of a subsolidus miscibility gap, or of the crystallographic parameters of the solid solution. The experimental method was "visual polythermal," which consists of heating samples to a constant temperature and making a visual observation to determine if complete melting has

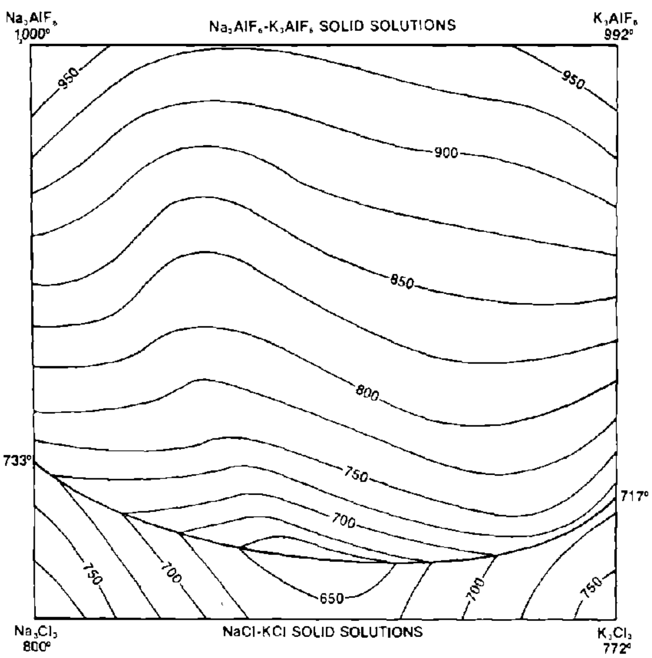

FIGURE 21. - The system $NaCl-KCl-Na_3AlF_6-K_3AlF_6$, redrawn from the data of reference 8.

occurred; if it has not, the temperature is increased and another observation is made, and this is continued until the sample appears to be completely liquid and the liquidus temperature is placed between the temperatures of the two final observations.

Three years later, Bukhalova (7) and Mal'tsev (36) presented crystallization data for Na_3AlF_6 and K_3AlF_6 in equilibrium with NaF, KF, NaCl, and KCl, indicating that there is no solid solution between Na_3AlF_6 and K_3AlF_6 but that elpasolite, K_2NaAlF_6, is present as a stoichiometric compound with a melting point of 932° C. To complicate the picture further, Edoyan (12), in the same year, reported six stoichiometric compounds between Na_3AlF_6 and K_3AlF_6: $2Na_3AlF_6 \cdot K_3AlF_6$; $5Na_3AlF_6 \cdot 3K_3AlF_6$; $Na_3AlF_6 \cdot K_3AlF_6$; $3Na_3AlF_6 \cdot 5K_3AlF_6$; $Na_3AlF_6 \cdot 2K_3AlF_6$; and $2Na_3AlF_6 \cdot 5K_3AlF_6$. Edoyan based the phase identification on the melting diagram and provided no characterization of the compounds. Edoyan also reported that addition of 14 to 15 wt pct K_3AlF_6 lowers the melting point of Na_3AlF_6 from 1,000° C to 832° C, almost 100° C below the lowest liquidus temperatures indicated by Mal'tsev (36).

The data of Mal'tsev are shown in figures 22-26. The crystallization volumes are described in terms of a compositional prism, the faces of which are shown by the three squares and two triangles of figure 22. Within the prism, they reported four stable crystallization tetrahedra:

$K_2NaAlF_6-Na_3AlF_6-Na_3F_3-Na_3Cl_3$

$K_2NaAlF_6-Na_3Cl_3-Na_3F_3-K_3Cl_3$

$K_2NaAlF_6-Na_3F_3-K_3Cl_3-K_3F_3$

$K_2NaAlF_6-K_3AlF_6-K_3Cl_3-K_3F_3$

They also provided liquidus diagrams for four ternary sections: $K_2NaAlF_6-Na_3F_3-K_3Cl_3$ (fig. 23); $K_2NaAlF_6-Na_3F_3-Na_3Cl_3$ (fig. 24); $K_2NaAlF_6-K_3F_3-Na_3Cl_3$

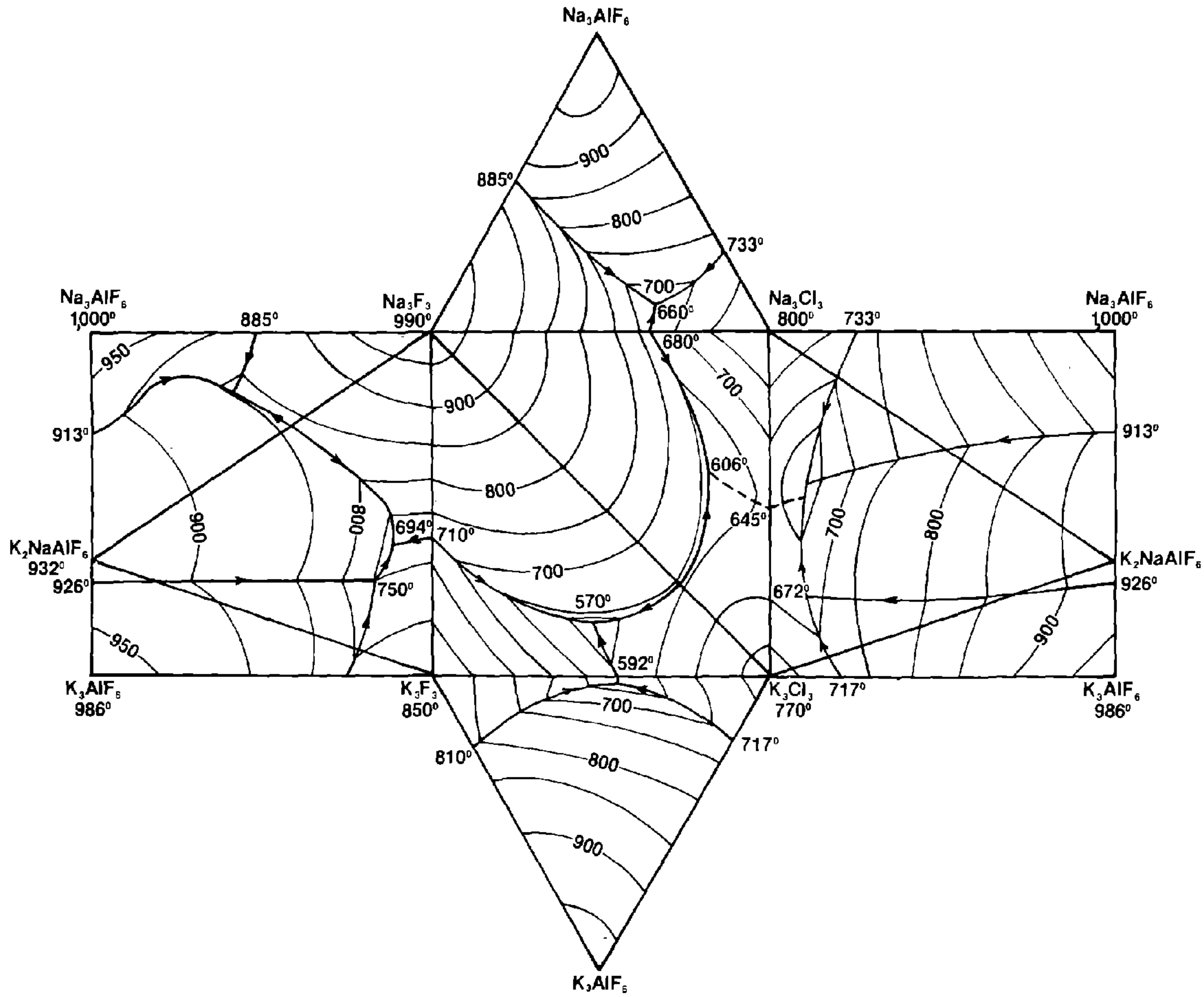

FIGURE 22. - Liquidus surfaces of the faces of the compositional prism for the system NaCl-KCl-NaF-KF-Na_3AlF_6-K_3AlF_6, redrawn from the data of reference 36.

(fig. 25); and K_2NaAlF_6-K_3F_3-K_3Cl_3 (fig. 26). None of the diagrams shows ternary equilibria, however. Figures 23, 24, and 26 show primary crystallization fields for K_3AlF_6 or Na_3AlF_6 even though they were described as "tetrahedrating sections." Figure 25 shows primary crystallization fields for both Na_3AlF_6 and K_3AlF_6 as well as for NaF. This indicates that the binary system KF-NaCl is not a true binary, and the existence of liquidus curves for NaCl and KF directly contradicts the data for that binary as shown in figure 22. It appears likely, therefore, that the primary crystallization fields are not well established and that the crystallizing phases were, in many cases, identified incorrectly.

The "diagonal reciprocal" relationships shown in figure 22 appear to be questionable; the Alkemade lines between K_2NaAlF_6 and the alkali halides cross phase boundaries in three of the four cases, with KCl, NaCl, and KF. This requires that elpasolite, K_2NaAlF_6, be a congruently melting phase in some sample compositions and an incongruently melting phase in others; this is possible only if elpasolite has a range of compositions. In view of the gently sloping liquidus surfaces, shallow phase boundary troughs, and inadequate characterization of the

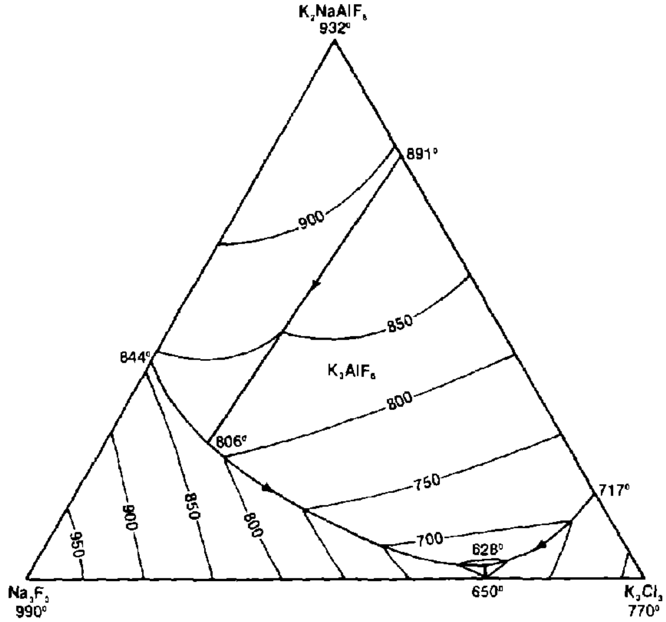

FIGURE 23. - The NaF-KCl-K_2NaAlF_6 section through the compositional prism shown in figure 22.

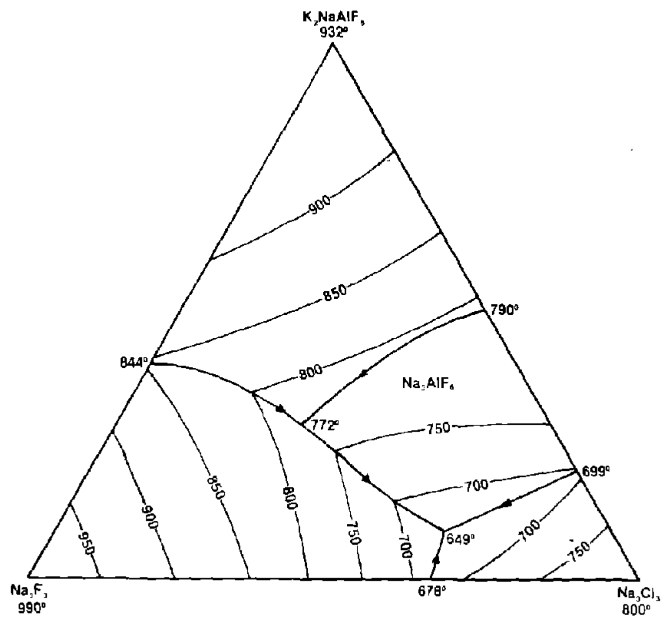

FIGURE 24. - The NaF-NaCl-K_2NaAlF_6 section through the compositional prism shown in figure 22.

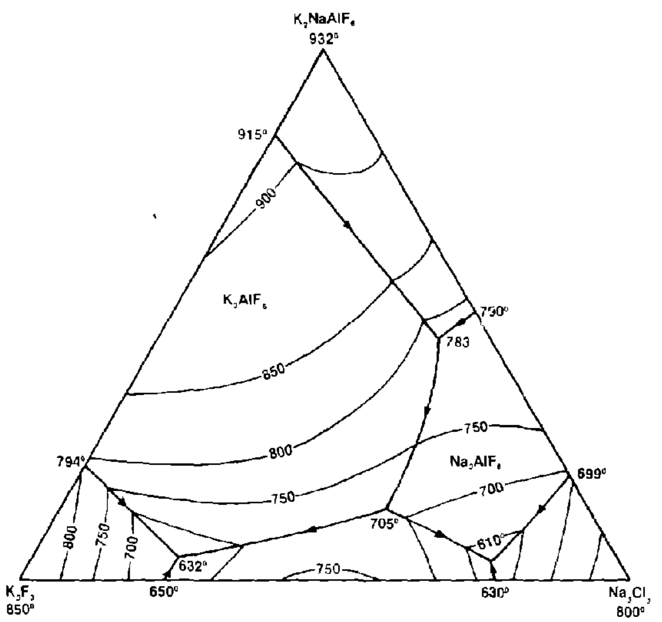

FIGURE 25. - The KF-NaCl-K_2NaAlF_6 section through the compositional prism shown in figure 22.

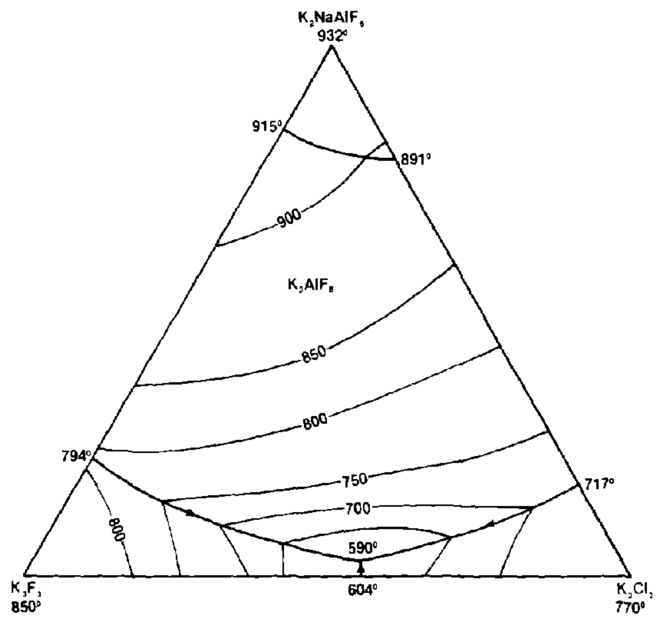

FIGURE 26. - The KF-KCl-K_2NaAlF_6 section through the compositional prism shown in figure 22.

crystalline phases, it is necessary to regard the data only as a general guide to aid in determination of temperatures of complete melting in the system.

Figure 27 shows the binary system Na_3AlF_6-K_3AlF_6, constructed from liquidus temperatures taken from figure 22 and solid solution information presented later in this report. The upper portion depicts an interpretation of the data, plotted on the same scale as binary diagrams shown earlier, to emphasize the flatness of the liquidus. The lower portion shows the same interpretation, expanded on the temperature axis to show the eutectics more clearly. The inset shows an alternative interpretation, with a peritectoid for the equilibrium among the limiting elpasolite solid solution, the limiting K_3AlF_6 solid solution, and liquid. This interpretation could account for incongruent melting of elpasolite in some cases. Some very meticulous experimental work would be necessary to determine relationships in this system.

The system studied by Mal'tsev (36) is not the complete system involved in formulation of aluminum fluxing salts because Na_3AlF_6 and K_3AlF_6 are not true components, being binary compounds of NaF and AlF_3 and of KF and AlF_6, respectively. It provides no information about melting temperatures in cases where AlF_3, $AlCl_3$, or other materials with Al-F ratios of <1:6 are added to the flux, for example. To provide a complete picture, the system must be defined as NaCl-KCl-$AlCl_3$-NaF-KF-AlF_3. Unfortunately, little information is available about this system other than that just described, which constitutes only a part of it.

As a first effort to provide such information, figure 28 shows a hypothetical ternary diagram of the system NaF-KF-AlF_3, constructed from the data of Bukhalova (36), which have been redrawn as a triaxial plot at the bottom, and from the data shown in figures 13, 15, and 16. To simplify the system and forego the uncertainty regarding the melting behavior of K_2NaAlF_6 or solid solutions thereof, the 750° C peritectic was changed to a eutectic in the subsystem K_2NaAlF_6-K_3AlF_6-KF;

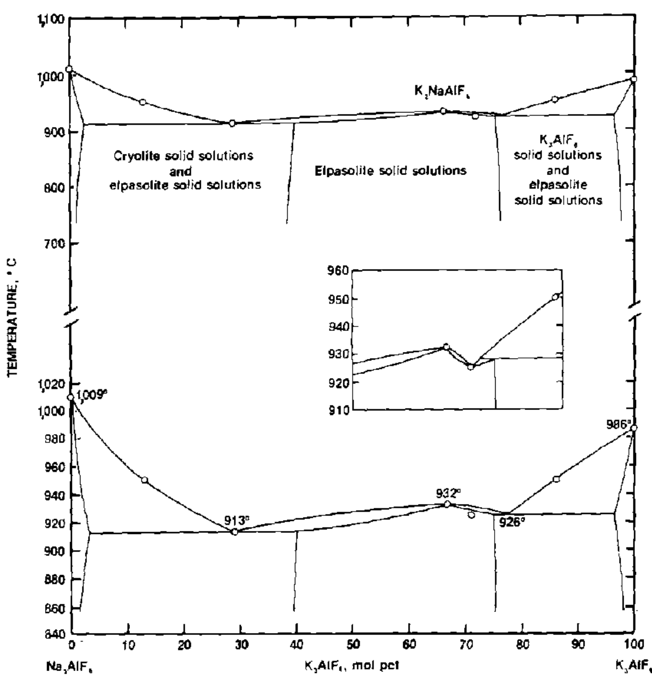

FIGURE 27. - The Na_3AlF_6-K_3AlF_6 binary diagram, drawn from ternary diagram of reference 36.

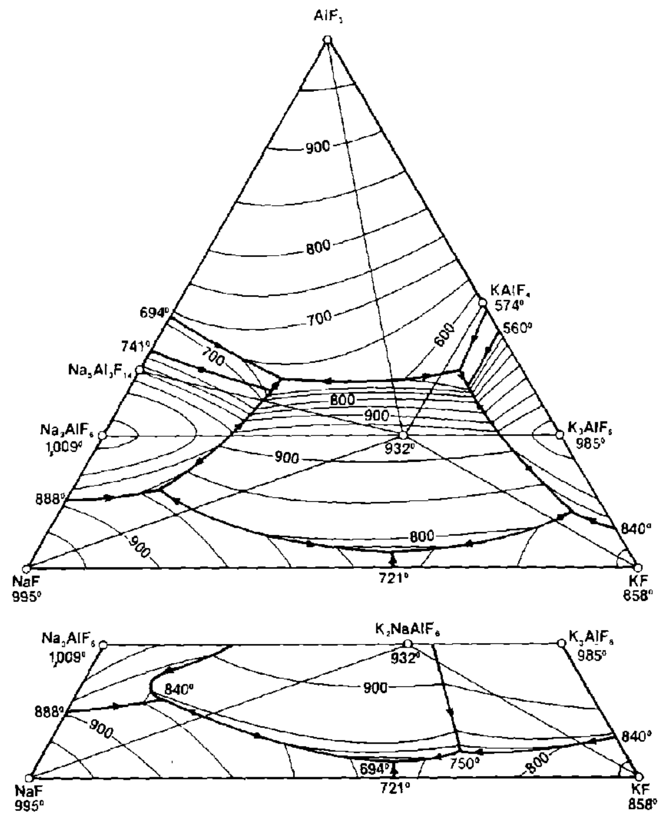

FIGURE 28. - The system NaF-KF-AlF_3. Lower diagram represents data of reference 36, redrawn as a triaxial graph. Upper diagram is hypothetical, based on binary equilibria data.

the phase boundaries within the subsystem K_2NaAlF_6-Na_3AlF_6-NaF were also changed to a more realistic, though hypothetical, configuration. Enough data are available to show that the Na_3AlF_6-K_3AlF_6 binary represents an important dividing line and that addition of AlF_3 to compositions along that line causes a very sharp decrease in liquidus temperatures and ternary eutectics below the 560° C and 694° C eutectics on the binaries.

Two other ternary diagrams within the system are available. The system NaCl-NaF-AlF_3 (29), shown in figure 29, indicates that NaCl-Na_3AlF_6 is a true binary and that addition of AlF_3 to mixtures of NaCl and Na_3AlF_6 can lower the liquidus temperature to a 626° C eutectic. Figure 30 shows that NaCl-KCl-NaF is a true ternary (51).

SUMMARY OF PHASE EQUILIBRIA DATA

The melting behavior of compositions in salts containing NaCl, KCl, $AlCl_3$, NaF, KF, and AlF_3 has not been thoroughly described in the literature; some generalizations are possible, however. It is noted, for example, that crystalline compounds with AlF_6 octahedral or alkali halide octahedral linkages are relatively stable, with high melting points and low vapor pressures, so that salt compositions within the volume bounded by NaCl, KCl, NaF, Na_3AlF_6, and K_3AlF_6 form reasonably stable melts. These compositions all have F-Al ratios >6. Addition of $AlCl_3$ or other phases with a F-Al ratio <6, however, lowers liquidus temperatures, drastically increases vapor pressures, and promotes hydrolysis. Relative stabilities of the crystalline compounds in the system indicate that the Al^{3+} ion is stable only in the AlF_6 octahedral configuration; in salts with F-Al ratios >6, the excess F^+ ions are bound strongly to Na^+ and K^+ ions, but in salts with F-Al ratios <6, the excess Al^{3+} ions form highly volatile aluminum chloride species, predominantly the neutral dimer Al_2Cl_6. In the system NaCl-KCl-$AlCl_3$-NaF-KF-AlF_3, therefore, the boundary between stable and unstable salt mixtures is the plane NaCl-KCl-Na_3AlF_6-AlF_6.

PHASE RELATIONS IN THE SYSTEM NaCl-KCl-$AlCl_3$-NaF-KF-AlF_3

Experimental research (57) has been carried out to address (1) the definition of the correct system in terms of subsolidus compatibility relationships and (2) the characterization of elpasolite in terms of its compositional range.

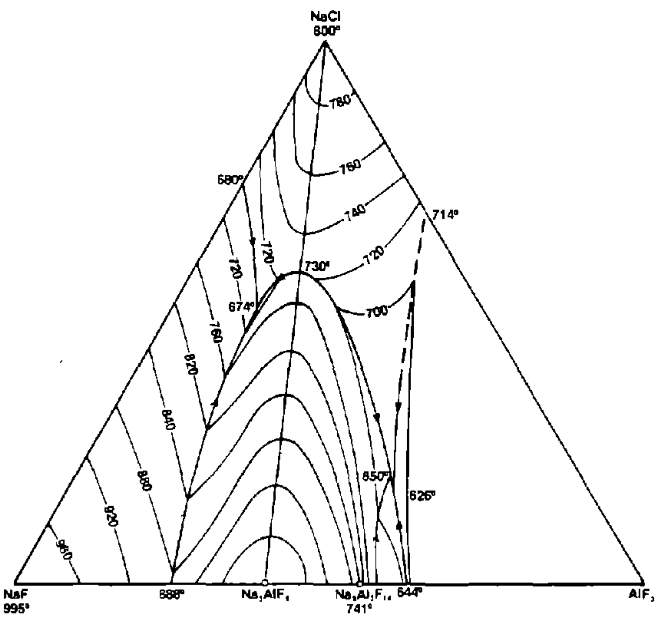

FIGURE 29. - The system NaCl-NaF-AlF_3, redrawn from the data of reference 29.

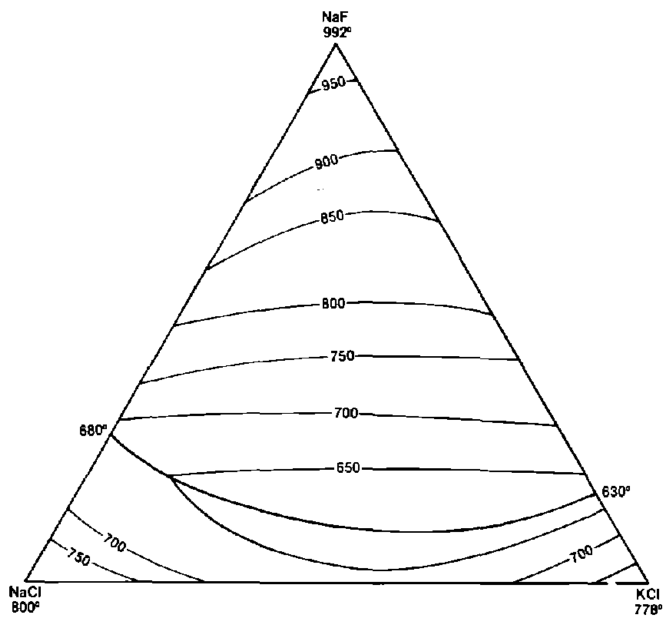

FIGURE 30. - The system NaCl-KCl-NaF, redrawn from the data of reference 51.

EXPERIMENTAL PROCEDURES

Reagent-grade NaCl, KCl, NaF, KF, and AlF_3 were dried in air at 350° C for at least 24 h prior to weighing and mixing. Anhydrous $AlCl_3$ was used as received. All chemicals were obtained from MCB Chemicals, Cincinnati, OH.[6] All compositions were prepared in 50-g batches, with each component weighed to the nearest 0.01 g, and were stored in airtight bottles. Only $AlCl_3$ and KF presented handling problems because of hydration in air. Special care was taken to weigh these components rapidly and to seal the samples immediately. For determination of subsolidus compatibility relationships, ~2-g samples of the compositions were sealed in evacuated borosilicate tubes and heated at 550°±10° C for 8 to 24 h. After heating, the tubes were cooled and broken, and the reacted samples were immediately pressed into pellets, using starch as a binder, and covered with plastic wrap to prevent absorption of moisture.

During the study, it was found that compositions with no free $AlCl_3$ or KF in the equilibrium assemblages could be melted in air without excessive vaporization losses and could be handled in air without moisture absorption, so several samples with the composition $KAlF_4$ and 16 samples on the Na_3AlF_6-K_3AlF_6 join were prepared by melting in air, in porcelain crucibles, and quenched by pouring the liquids into a stainless steel beaker immersed in water. The quenched samples were ground with mortar and pestle and annealed in air at 800° C.

Phases in the covered samples were identified by X-ray diffractometry, using CuKα radiation at a scanning rate of 1° 2θ per minute. Detailed X-ray data for $KAlF_4$ and the quenched and annealed samples on the Na_3AlF_6-K_3AlF_6 join were obtained by scanning at 0.25° 2θ per minute, using a quartz internal standard for precision measurement of diffraction angles. Intensities of the diffraction lines were measured by counting squares under the recorded diffraction peaks.

SOLID SOLUBILITY IN THE ELPASOLITE PHASE

The essentially identical structures of cryolite, elpasolite, and K-cryolite seem to be amenable to accommodation of variable amounts of cations of different sizes through slight distortions of the anion network and symmetry changes. This speculation, coupled with the importance of the cryolite series in crystallized fluxing salts, prompted a study of the solid solubility limits in the system Na_3AlF_6-K_3AlF_6. Detailed lattice and intensity measurements of the 16 compositions quenched from the melts and annealed at 800° C are shown in figures 31 and 32. The limited number of samples and the scatter in the lattice measurements do not permit accurate determination of solubility limits, but the data show rather sharp changes in the parameters of cryolite and K-cryolite,

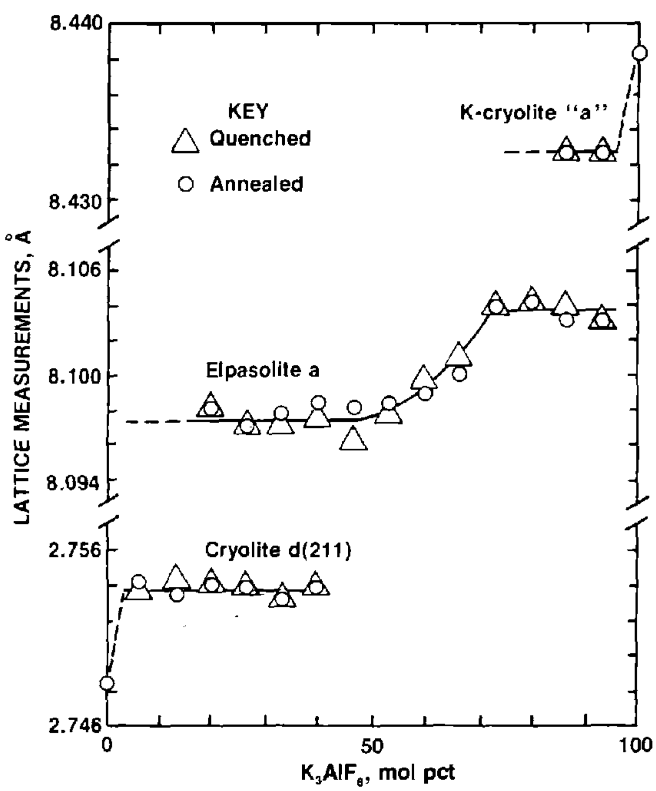

FIGURE 31. - X-ray lattice measurements for samples in the system Na_3AlF_6-K_3AlF_6.

[6]Reference to specific products does not imply endorsement by the Bureau of Mines.

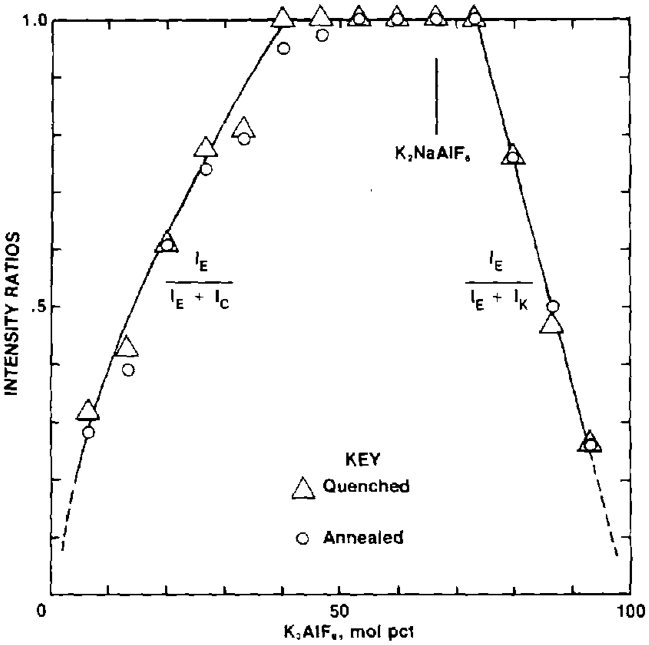

FIGURE 32. - X-ray intensity ratio measurements for samples in the system Na_3AlF_6-K_3AlF_6.

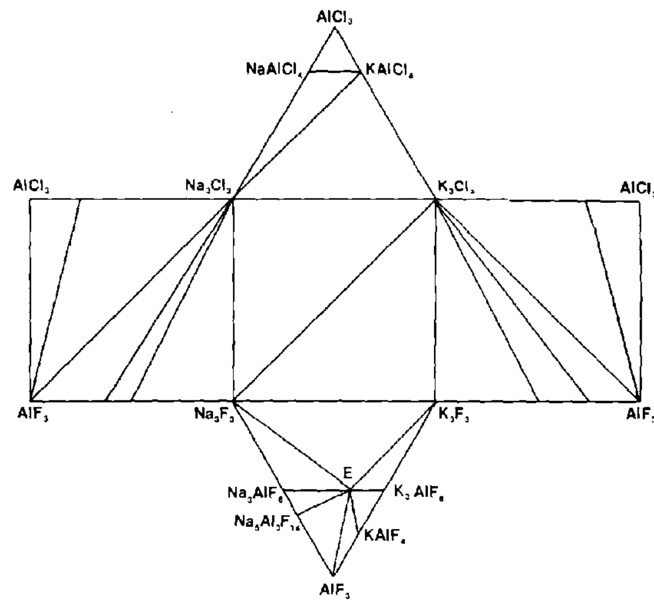

FIGURE 33. - Surfaces of the compositional prism for the system $NaCl$-KCl-$AlCl_3$-NaF-KF-AlF_3, showing subsolidus compatibility relationships.

indicating mutual solubility of <5 mol pct in the end members. The intensity ratios provide a more reliable estimate of the solubility limits in elpasolite, whose compositional range is placed between 40±5 mol pct and 75±5 mol pct K_3AlF_6. The ratios for the annealed samples are not significantly different from those of the quenched samples, so it is concluded that no appreciable unmixing occurs at 800° C or at room temperature.

It might be expected that limited solubility occurs in the $NaAlCl_4$-$KAlCl_4$ series and that there is limited solubility in $KAlF_4$ and $Na_5Al_3F_{14}$, but these solubilities have not been determined. There is also a possibility of chloride-fluoride substitution, but this has not been studied.

SUBSOLIDUS EQUILIBRIA

To determine the order of the system $NaCl$-KCl-$AlCl_3$-NaF-KF-AlF_3, it was necessary to identify the irreversible exchange reactions between mixed halides. X-ray analyses of reaction products formed in sealed evacuated tubes showed the following binary reactions:

$$NaCl + KF \rightarrow NaF + KCl \quad (1)$$

$$3\ NaF + AlCl_3 \rightarrow 3\ NaCl + AlF_3 \quad (2)$$

$$3\ KF + AlCl_3 \rightarrow 3\ KCl + AlF_3 \quad (3)$$

Reaction 1 verifies previous work (25, 36, 47). Reactions 2 and 3 indicate reciprocal systems which, coupled with the chloride and fluoride ternaries, show that all phases and crystallization volumes can be represented graphically within a trigonal compositional prism whose faces are shown in figure 33. Once the reciprocal diagonals were established, the other tie lines were fixed by geometric necesssity, as shown.

The following binary reactions were also observed to occur in three component mixtures:

$$KCl + NaCl + AlCl_3 \rightarrow NaCl + KAlCl_4 \quad (4)$$

$$NaF + 2KF + 2AlF_3 \rightarrow AlF_3 + K_2NaAlF_6 \quad (5)$$

Reaction 4 fixes the binary joins in the chloride ternary as $NaAlCl_4$-$KAlCl_4$ and $NaCl$-$KAlCl_4$, and reaction 5, coupled with previous work (13), fixes the binary joins in the fluoride ternary as shown in figure 3. These were verified by subsequent experimental determination of the resulting quaternary assemblages.

To establish the binary joins within the compositional prism, the following ternary reactions were verified experimentally:

$$2NaF + 3KF + AlF_3 \rightarrow NaF + KF + K_2NaAlF_6 \qquad (6)$$

$$5NaCl + 5KCl + NaF + 2KF + AlF_3 \rightarrow 4NaCl + 5KCl + K_2NaAlF_6 \qquad (7)$$

$$KCl + NaF + 4KF + AlF_3 \rightarrow KCl + 2KF + K_2NaAlF_6 \qquad (8)$$

In addition, six compositions with different percentages of NaCl, KCl, and AlF_3 were heated in sealed tubes and were found to undergo no net reaction. Reactions 6, 7, and 8 establish the existence of stable joins between elpasolite, K_2NaAlF_6, and the component alkali halides. This, coupled with the proven existence of NaCl-KCl-AlF_3 as a stable ternary, requires that the compositional prism be divided into 12 compatibility tetrahedra, as shown in figure 34. To verify those conclusions, 12 compositions, one each within the 12 tetrahedra, were prepared and reacted in sealed evacuated tubes. For ease of visualization, the prism has been divided into three volumes, as illustrated in figures 35-37, and indicated below. The reactions observed follow:

1. $NaCl + 7KF + 2AlF_3 \rightarrow KCl + KF + K_3AlF_6 + K_2NaAlF_6$ (9)
2. $2NaCl + 5KF + AlF_3 \rightarrow 2KCl + NaF + KF + K_2NaAlF_6$ (10)
3. $3KCl + 4NaF + AlF_3 \rightarrow 2NaCl + NaF + KCl + K_2NaAlF_6$ (11)
4. $2KCl + 7NaF + 2AlF_3 \rightarrow 2NaCl + NaF + Na_3AlF_6 + K_2NaAlF_6$ (12)
5. $NaCl + 7KF + 3AlF_3 \rightarrow KCl + KAlF_4 + K_3AlF_6 + K_2NaAlF_6$ (13)
6. $2KCl + 11NaF + 5AlF_3 \rightarrow 2NaCl + Na_3AlF_6 + Na_5Al_3F_{14} + K_2NaAlF_6$ (14)
7. $NaCl + 4NaF + 3AlF_3 \rightarrow KCl + AlF_3 + KAlF_4 + K_2NaAlF_6$ (15)
8. $2KCl + 8NaF + 5AlF_3 \rightarrow 2NaCl + AlF_3 + Na_5Al_3F_{14} + K_2NaAlF_6$ (16)
9. $NaCl + NaF + 2KF + 2AlF_3 \rightarrow NaCl + KCl + AlF_3 + K_2NaAlF_6$ (17)
10. $NaCl + 2KCl + AlCl_3 + AlF_3 \rightarrow NaCl + KCl + AlF_3 + KAlCl_4$ (18)
11. $2NaCl + KCl + 2AlCl_3 + AlF_3 \rightarrow AlF_3 + NaCl + NaAlCl_4 + KAlCl_4$ (19)
12. $NaCl + KCl + 3AlCl_3 + AlF_3 \rightarrow AlCl_3 + AlF_3 + NaAlCl_4 + KAlCl_4$ (20)

As a further aid to visualization, figure 38 shows the 12 tetrahedra in a section through the center of the prism; in this representation, points represent binary assemblages, lines represent ternary assemblages, and triangles or parallelograms represent quaternary assemblages. The tetrahedra are numbered in accordance with the numbers of the reactions listed above.

Tetrahedra 1-4 confirm the subsolidus compatibility reported by Mal'tsev (<u>36</u>). Tetrahedra 5-12 have been determined for the first time (<u>57</u>).

POWDER DIFFRACTION DATA FOR $KAlF_4$ AND K_3AlF_6

There is some diagreement regarding the symmetry of $KAlF_4$. Brosset (5)

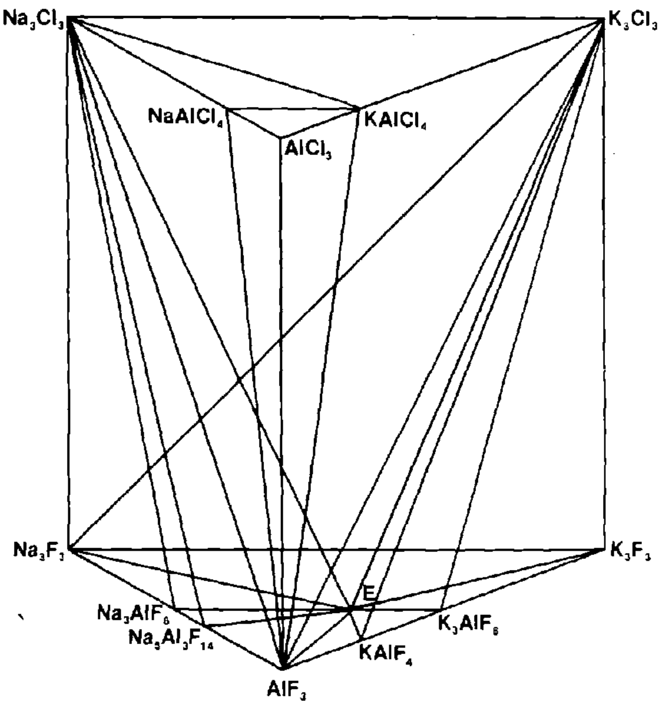

FIGURE 34. - Subsolidus compatibility tetrahedra in the system NaCl-KCl-$AlCl_3$-NaF-KF-AlF_6.

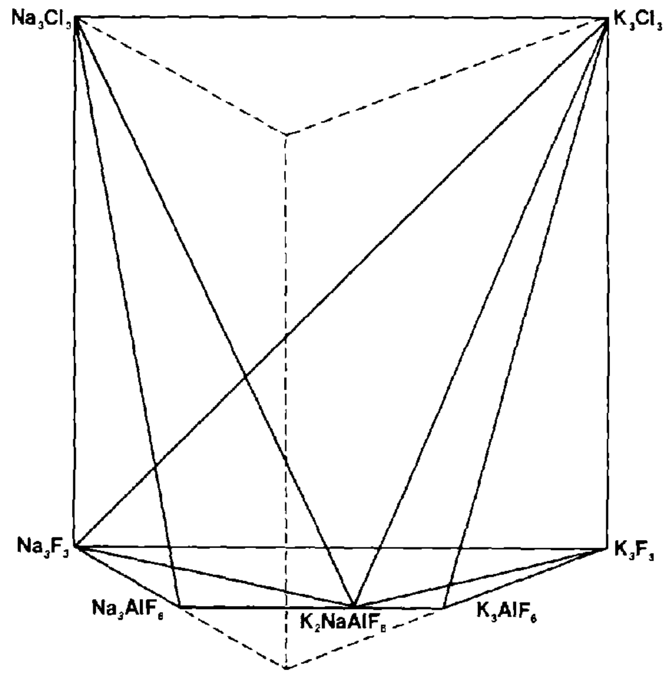

FIGURE 35. - Subsolidus compatibility in the portion of the system NaCl-KCl-$AlCl_3$-NaF-KF-AlF_3 corresponding to those in reference 36.

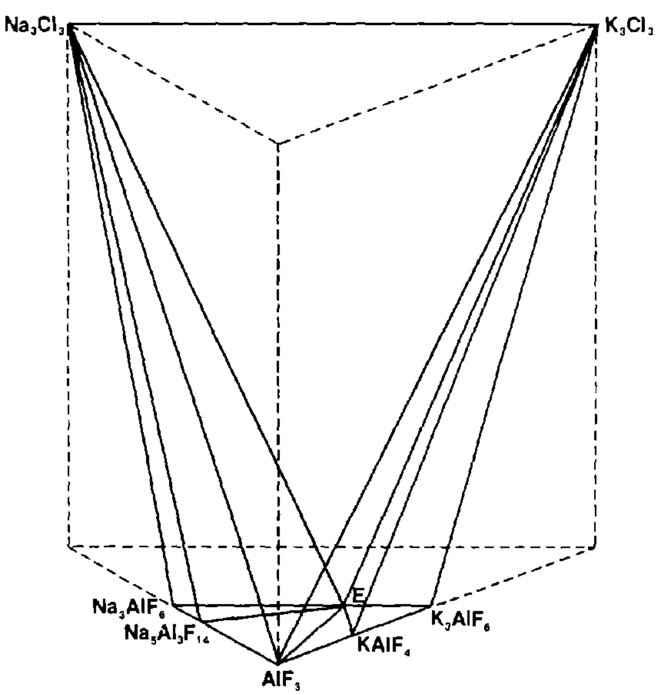

FIGURE 36. - Subsolidus compatibility tetrahedra in the volume bounded by NaCl-KCl-AlF_3-Na_3AlF_6-K_3AlF_6.

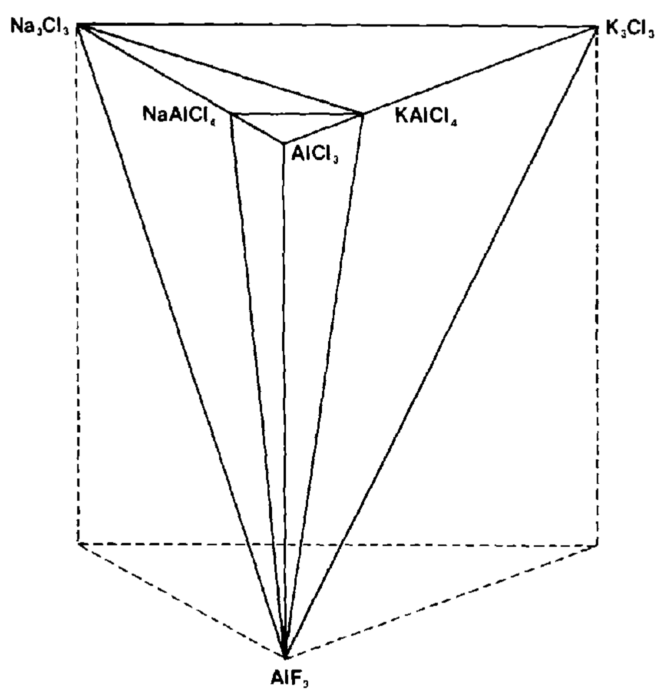

FIGURE 37. - Subsolidus compatibility tetrahedra in the volume bounded by NaCl-KCl-$AlCl_3$-AlF_3.

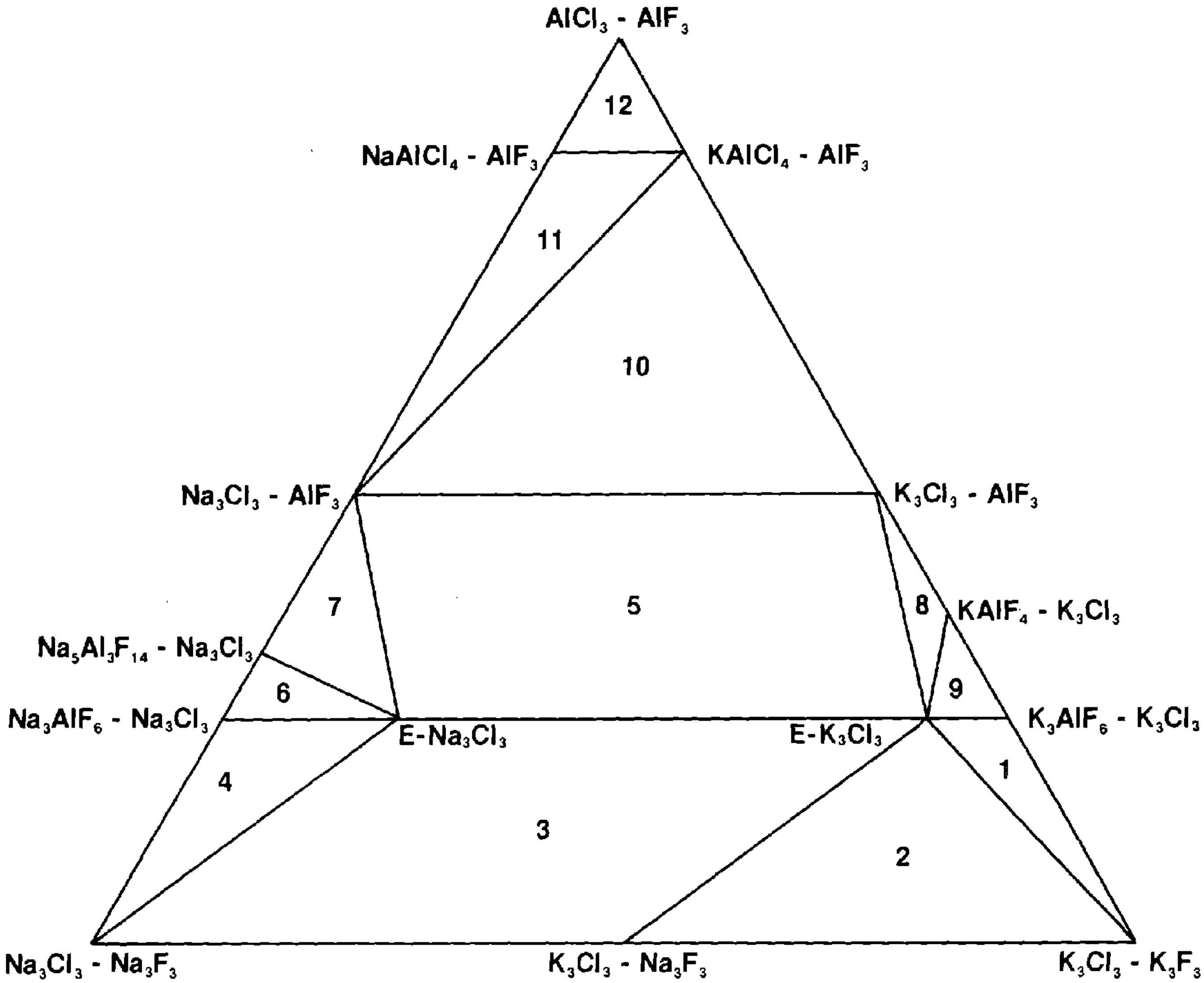

FIGURE 38. - Section through the compositional prism of the system NaCl-KCl-$AlCl_3$-NaF-KF-AlF_3 at the chloride-fluoride molar ratio of 1:1.

originally assigned it to the tetragonal system and determined the structure on that basis. Phillips (44), however, reported the symmetry as orthorhombic at low temperatures, with a reversible transition to cubic at about -15° C. Grjotheim (17) reported it to be tetragonal, with a transition to cubic at 327° C. The powder data obtained in this study indicate tetragonal symmetry; because the data in the Powder Diffraction file are incomplete, detailed data are listed in table 10, along with calculated intensities based on Brosset's structure. The calculated and observed intensities are in sufficiently good agreement to indicate that the reported structure is essentially correct.

The tetragonal symmetry of K_3AlF_6 at 25° C as reported by Steward (59), with unit cell parameters as in table 1, was confirmed by this study.

CONCLUSIONS

Available data on crystal structures, powder diffraction data, and phase equilibria data for the entire system NaCl-KCl-$AlCl_3$-NaF-KF-AlF_3 have been assembled into one publication. Bureau of Mines determination of the subsolidus

TABLE 10. - Powder diffraction data for $KAlF_4$

hkl	Calculated[1]		PDF card 2-595		Observed	
	d, Å	I	d, Å	I	d, Å	I
001	6.155	8.1	NR	NR	6.146	9.8
100	3.570	12.3	3.57	20	3.570	6.6
101	3.088	71.1	3.08	100	3.084	100.0
002	3.077	28.9				
110	2.525	28.4	2.52	50	2.525	27.4
111	2.336	40.3	2.32	70+	2.333	53.8
102	2.331	23.4				
003	2.051	4.6	NR	NR	2.051	5.5
112	1.952	.1	NR	NR	ND	ND
200	1.785	41.0	1.779	100	1.782	82.3
103	1.779	34.8				
201	1.714	1.0	NR	NR	ND	ND
210	1.597	1.7	NR	NR	NM	3.9
113	1.592	.9	NR	NR	ND	ND
211	1.546	16.9	1.540	70	1.542	57.1
202	1.544	12.6				
004	1.539	22.0	1.538	50		
212	1.417	5.5	NR	NR	NM	3.2
104	1.413	.1	NR	NR	ND	ND
203	1.347	3.1	NR	NR	NM	2.4
114	1.314	3.7	1.313	20	NM	4.3
220	1.262	10.1	1.258	70	1.260	25.2
213	1.260	18.6				
221	1.236	.2	NR	NR	ND	ND
005	1.231	<.1	NR	NR	ND	ND
300	1.190	1.3	NR	NR	ND	ND
301	1.168	3.1	1.165	50	ND	ND
222	1.168	.2				
204	1.165	11.8	1.163	50+	1.166	15.7
105	1.164	1.3				
310	1.129	3.8	NR	NR	NM	5.6

d = interplanar spacing; I = X-ray diffraction intensity; ND = not detected; NM = not measurable with precision; NR = not reported.

[1]Spacings calculated for a = 3.570 Å; c = 6.154 Å at 22° C. Relative intensities calculated for z = 0.21, with no temperature correction.

compatibility relationships provides quidelines for systematic research into the properties of molten salts in the system.

Based on information in the literature, the compatibility relationships described in this work, and observations made during the research, the system can be divided into three distinct crystallization volumes. Compositions within each of the volumes will melt to form molten salts with properties within ranges quite different from those in the other volumes. Molten salts within the volume bounded by NaCl, KCl, NaF, KF, Na_3AlF_6, and K_3AlF_6 (fig. 35) are relatively stable, with high melting points and low vapor pressures; these salts have a F-Al ratio >6 so that all the Al^{3+} ions are in stable AlF_6 octahedra. Detailed property determinations are needed for a thorough understanding of the relationships among salt composition, molten salt structures, properties, and fluxing efficiencies.

Molten salts within the volume bounded by NaCl, KCl, AlF_3, Na_3AlF_6, and K_3AlF_6, shown in figure 36, are considerably less stable, with lower melting points and higher vapor pressures. The stable crystalline phases within the volume are

NaCl, KCl, and all the fluorides of aluminum and the alkalies; the F-Al ratio is <6 and, though the Al^{3+} ion can be in octahedral coordination, the melting temperatures and other properties depend on the interactions of the alkali ions and the AlF_6 octahedra.

Molten salts within the volume bounded by NaCl, KCl, $AlCl_3$, and AlF_3, shown in figure 37, crystallize to form only one stable fluoride, AlF_3, which is a volatile phase, along with the even more volatile phases $AlCl_3$, $NaAlCl_4$, and $KAlCl_4$. The F-Al ratio is <3, and the Al^{3+} ions necessarily are forced into unstable coordination with the halide ions.

Very little information on molten salt properties within the volumes shown in figures 36 and 37 is available in the literature. In fact, density, vapor pressure, surface tension, and viscosity data are virtually nonexistent except for some of the binary assemblages.

Because deliberate additions are commonly made to aluminum fluxing salts, differential vaporization and hydrolysis reactions can change salt compositions during use, and reactions with components of the scrap can alter chemistry, it is essential that the entire system be characterized in terms of properties.

REFERENCES

1. Baenziger, N. C. The Crystal Structure of $NaAlCl_4$. Acta. Cryst., v. 4, 1951, pp. 216-219.

2. Barton, C. J., L. M. Bratcher, and W. R. Grimes. The System NaCl-KCl-$AlCl_3$. Paper in Phase Diagrams of Nuclear Reactor Materials, ed. by R. E. Thoma. Oak Ridge Natl. Lab. Rep., ORNL-2548, 1959, p. 32.

3. Bragg, W. L. The Structure of Some Crystals as Indicated by Their Diffraction of X-Rays. Proc. Roy. Soc. (London), ser. A, v. 89, 1913, pp. 248-277.

4. Brosset, C. Crystal Structure of Chiolite. Z. Anorg. Allgem. Chem., v. 238, 1938, pp. 201-208.

5. _____. Preparation and Crystal Structure of a Few Alkali Aluminum Fluorides of the Type $TlAlF_4$. Z. Anorg. Allgem. Chem., v. 239, 1938, pp. 301-304.

6. _____. Potassium Cryolite, a Complex Compound With a Variable Composition. Ark. Kemi, Mineral. Geol., v. 21A, 1946, pp. 1-9.

7. Bukhalova, G. A., G. N. Maslennikova, and D. M. Rabkin. (Ternary System of Chlorides and Hexafluoroaluminates of Sodium and Potassium.) Zh. Neorg. Khim., v. 7, 1962, pp. 1640-1643.

8. Bukhalova, G. A., and V. T. Mal'tsev. (System of Sodium and Potassium Fluorides and Hexafluoroaluminates.) Zh. Neorg. Khim., v. 10, 1965, pp. 189-193.

9. Chikanov, N. D., A. P. Palkin, and M. K. Bizyaeva. (Thermal Study of the Systems Na, K‖ $AlCl_4$, $Ta(Nb)Cl_6$.) Zh. Neorg. Khim., v. 8, 1963, pp. 1938-1944.

10. Cochran, C. N. Calculated Model for NaF-AlF_3 System. Trans. AIME, v. 239, 1967, pp. 1056-1059.

11. Coleman, D. S., and P. D. A. Lacy. The Phase Equilibrium Diagram for the KCl-NaCl System. Mater. Res. Bull., v. 2, 1967, pp. 935-938.

12. Edoyan, R. S., M. G. Manvelyan, and G. G. Babayan. (Physicochemical Study of the Systems Containing Na_3AlF_6, K_3AlF_6, and Li_3AlF_6. I. Melting Diagram of the Na_3AlF_6-K_3AlF_6 System.) Izv. Akad. Nauk. Arm. SSR, Khim. Nauki, v. 18, 1965, pp. 10-14.

13. Foster, P. A., Jr. Phase Equilibria in the System Na_3AlF_6-AlF_3. J. Am. Ceram. Soc., v. 53, 1970, pp. 598-600.

14. Fuseya, G., C. Sugihara, N. Nagao, and I. Teraoka. Measurements of the Freezing Points in the System Cryolite-Sodium Fluoride-Alumina. J. Electrochem. Soc. Japan, v. 18, 1950, pp. 65-67.

15. Garton, G., and B. M. Wanklyn. Some Observations on the Tetrafluoroaluminates of Lithium and Sodium. J. Inorg. Nucl. Chem., v. 27, 1965, pp. 2461-2465.

16. Gillett, H. W., and G. M. James. Melting Aluminum Chips. BuMines B 108, 1916, 88 pp.

17. Grjotheim, K. The Theory of Aluminum Electrolysis. Kgl. Nor. Vidensk. Selsk. Skr., v. 2, 1957, pp. 1-90.

18. Grjotheim, K., T. Halvorsen, and J. L. Holm. The Phase Diagram of the System NaF-NaCl and Thermodynamic Properties of Fused Mixtures. Acta Chem. Scand., v. 21, 1967, pp. 2300-2301.

19. Grothe, H., and C. A. Piel. Fusion of Salts for Aluminum Chloride Hydrolysis. Z. Elektrochem. Angew. Phys. Chem., v. 54, 1950, pp. 210-215.

20. Hanawalt, J. D., H. W. Rinn, and L. K. Frevel. Chemical Analysis by X-ray Diffraction. Classification and Use of X-ray Diffraction Patterns. Ind. and Eng. Chem., Anal. Ed., v. 10, 1939, pp. 457-512.

21. Helmholtz, L. Paramagnetic Resonance Spectrum of the Fluoferrate Ion, FeF_6^{3-}. J. Chem. Phys., v. 31, 1959, pp. 172-175.

22. Holm, J. L. Phase Transitions and Structure of High-Temperature Phases of Some Compounds of the Cryolite Family. Acta Chem. Scand., v. 19, 1965, pp. 261-263.

23. _____. Phase Relations in the Systems NaF-LiF, NaF-KF, and NaF-RbF. Acta Chem. Scand., v. 19, 1965, pp. 638-644.

24. Howard, E. H. Some Physical and Chemical Properties of a New Sodium Aluminum Fluoride. J. Am. Chem. Soc., v. 76, 1954, pp. 2041-2042.

25. Ishaque, M. (Liquid-Solid Equilibria in the Quaternary System Containing NaCl, KCl, $CaCl_2$, NaF, KF, CaF_2.) Bull. Soc. Chim. France, Nos. 1-2, 1952, pp. 127-138.

26. Kendall, J., E. D. Crittenden, and H. K. Miller. A Study of Factors Influencing Compound Formation and Solubility in Fused Salt Systems. J. Am. Chem. Soc., v. 45, 1923, pp. 963-996.

27. Ketelaar, J. A. A. The Crystal Structures of the Aluminum Halides. I. The Structure of Aluminum Trifluoride. Z. Kristallogr., v. 85, 1933, pp. 119-131.

28. Ketelaar, J. A. A., C. H. MacGillavry, and P. A. Renes. The Crystal Structure of Aluminum Chloride. Rec. Trav. Chim., v. 60, 1947, pp. 501-512.

29. Kuvakin, M. A., and P. S. Kusakin. (The Sodium Fluoride-Aluminum Fluoride-Sodium Chloride System.) Zh. Neorg. Khim., v. 4, 1959, pp. 2577-2581.

30. Levin, E. M., J. F. Kenny, R. D. Wells, and J. T. Benedict. System Sodium Chloride-Aluminum Chloride. J. Res. NBS, sec. A, v. 78, 1974, pp. 505-507.

31. Levin, E. M., and H. F. McMurdie. Phase Diagrams for Ceramists. Figures 4150-4999. Am. Ceram. Soc., Columbus, OH, 1975, 513 pp.

32. Levin, E. M., C. R. Robbins, and H. F. McMurdie. Phase Diagrams for Ceramists. Figures 1-2066. Am. Ceram. Soc., Columbus, OH, 1964, 601 pp.

33. _____. Phase Diagrams for Ceramists. Figures 2067-4149. Am. Ceram. Soc., Columbus, OH, 1969, 625 pp.

34. Magyar, M. J., R. S. Kaplan, and H. V. Makar. Experimental Processing of Salt Slags From an Aluminum Dross Furnace. BuMines RI 8446, 1980, 26 pp.

35. Majumdar, A. J., and R. Roy. Test of the Applicability of the Clapeyron Relation to a Few Cases of Solid-Solid Transitions. J. Inorg. Nucl. Chem., v. 27, 1965, pp. 1961-1973.

36. Mal'tsev, V. T., and G. A. Bukhalova. Reciprocal System of Fluorides, Chlorides, and Hexafluoroaluminates of Sodium and Potassium. Zh. Neorg. Khim., v. 10, 1965, pp. 797-800.

37. Mashovets, V. P., M. S. Beletskii, Y. G. Saksonov, and R. V. Svoboda. A New Compound in the System $NaF-AlF_3$. Dokl. Akad. Nauk SSSR, v. 113, 1957, pp. 1290-1292.

38. Menzer, G. Crystal Srtucture of the Cryolite Group. Fortschr. Mineral. Kristallogr. Petrog., v. 17, 1932, p. 439.

39. Mesrobian, G., M. Rolin, and H. Pham. (Study Under Pressure of Sodium Fluoride-Aluminum Fluoride Mixtures, Rich in Aluminum Fluoride.) Rev. Int. Hautes Temp. Refract., v. 9, 1972, pp. 139-146.

40. Midorikawa, R. Electrolytic Purification of Aluminum At Low Temperature in Aluminum Chloride Baths. I. Eutectic

Points of Aluminum Chloride-Sodium Chloride and Aluminum Chloride-Potassium Chloride Baths. J. Electrochem. Soc. Japan, v. 23, 1955, pp. 72-76.

41. Midorikawa, R. Electrolytic Refining of Aluminum. II. The Melting Point of the System $AlCl_3$-NaCl-KCl. J. Electrochem. Soc. Japan, v. 23, 1955, pp. 127-129.

42. Morris, M. C., H. F. McMurdie, E. H. Evans, B. Paretzkin, and J. H. deGroot. Standard X-ray Diffraction Powder Patterns. NBS Monog. 25, sec. 16, 1979, p. 63.

43. Naray-Szabo, S., and K. Sasvari. The Crystal Structure of Cryolite, Na_3AlF_6. Z. Kristallogr., v. 99A, 1938, pp. 27-31.

44. Phillips, B., C. M. Warshaw, and I. Mockrin. Equilibria in $KAlF_4$-Containing Systems. J. Am. Ceram. Soc., v. 49, 1966, pp. 631-634.

45. Phillips, N. W. F., R. H. Singleton, and E. A. Hollingshead. Liquidus Curves for Aluminum Cell Electrolytes. I. Cryolite-Alumina. J. Electrochem. Soc., v. 102, 1955, pp. 648-649.

46. ______. Liquidus Curves for Aluminum Cell Electrolytes. II. Ternary Systems of Cryolite-Alumina With Sodium Fluoride, Sodium Chlorides, and Aluminum Fluoride. J. Electrochem. Soc., v. 102, 1955, pp. 690-692.

47. Polyakov, V. D. (Double Decomposition in the Absence of a Solvent. LIV. Quaternary Mutual Solution: Fluorides, Bromides, and Chlorides of Sodium and Potassium.) Izv. Sektora Fiz.-Khim. Anal., Inst. Obshch. Neorg. Khim., Akad. Nauk SSSR, v. 13, 1940, pp. 299-320.

48. Posnjak, E., and R. W. G. Wyckoff. The Crystal Structures of the Alkali Halides. J. Wash. Acad. Sci., v. 12, 1922, pp. 248-251.

49. Rao, S., and P. R. Dawson. A State-of-the-Art Report on Secondary Aluminum Processes With Particular Emphasis on Fluxes and Emission Control. Warren Spring Lab., Dep. Industry, Stevenage, U.K., Rep. LR 359 (ME), June 1980, 82 pp.

50. Ruff, O., and L. LeBoucher. (The Vapor Pressures of Zinc, Cadmium, Magnesium, Calcium, Strontium, Barium, and Aluminum Fluorides.) Z. Anorg. Allgem. Chem., v. 219, 1934, pp. 376-381.

51. Sauerwald, F., and H. E. Dombois. (The General Forms of a Ternary Diagram With Two Binary Systems With Eutectics and One System With a Minimum Temperature and a Critical Solution Temperature, Such as the System KCl-NaCl-NaF.) Z. Anorg. Allgem. Chem., v. 277, 1954, pp. 62-72.

52. Scheil, E., and H. Stadelmaier. (Segregation in Potassium Chloride-Sodium Chloride Solid Solutions.) Z. Metallk., v. 43, 1956, pp. 227-236.

53. Semenenko, K. N., V. N. Surov, and N. S. Kedrova. (Synthesis and Study of Alkali Metal and Ammonium Chloroaluminates.) Zh. Neorg. Khim., v. 14, 1969, pp. 923-927.

54. Shinn, D. B., D. S. Crockett, and H. M. Haendler. The Thermochemical Decomposition of Ammonium Hexafluoroferrate(III) and Ammonium Hexafluoroaluminate. A New Crystalline Form of AlF_3. Inorg. Chem., v. 5, 1966, pp. 1927-1929.

55. Shvartsman, V. I. Thermal Analysis of the Systems $AlCl_3$-NaCl and $AlCl_3$-KCl. Zap. Inst. Khim., Akad. Nauk SSSR, v. 7, 1940, pp. 3-9.

56. Smits, A., and J. L. Meijering. The Complexity of Aluminum Chloride. Z. Physik. Chem., v. B41, 1938, pp. 38-111.

57. Sorrell, C. A., and J. G. Groetsch, Jr. Phase Relations in the System NaCl-KCl-$AlCl_3$-NaF-KF-AlF_3. J. Am. Ceram. Soc., 1986.

58. Staritzky, E., and L. B. Asprey. Crystallographic Data. 159. Aluminum Trifluoride, AlF_3. Anal. Chem., v. 29, 1957, pp. 984-985.

59. Steward, E. G., and H. P. Rooksby. Transitions in Crystal Structure of Cryolite and Related Fluorides. Acta Crystallogr., v. 6, 1953, pp. 49-52.

60. Sully, A. H., H. K. Hardy, and T. J. Heal. An Investigation of Thickening and Metal Entrapment in a Light Metal Alloy Melting Flux. J. Inst. Met., v. 82, 1953-54, pp. 49-58.

61. Swanson, H. E., and R. K. Fuyat. Standard X-ray Diffraction Powder Patterns. NBS. Circ. 539, v. II, 1953, pp. 41-43.

62. Swanson, H. E., H. F. McMurdie, M. C. Morris, E. H. Evans, and B. Paretzkin. Standard X-ray Diffraction Powder Patterns. NBS. Monog. 25, sec. 9, 1971, pp. 43, 61-62.

63. Swanson, H. E., and E. Tatge. Standard X-ray Diffraction Powder Patterns. NBS. Circ. 539, v. 1, 1953, pp. 63-66.

64. Witt, W. P., and R. F. Barrow. Heat of Sublimation of Aluminum Fluoride and the Heat of Formation of Aluminum Monofluoride. Trans. Faraday Soc., v. 55, 1959, pp. 730-735.

65. Zhemchuzhina, E. A., and A. I. Belyaev. Surface Phenomenon and the Adsorption of Aluminum Oxides by Fluxes. Sb. Nauch n. Tr. Mosk. Inst. Tsvetn. Met. i Zolota, No. 31, 1958, pp. 131-143.

66. _____. Interphase Tension of Liquid Aluminum at the Boundary With Molten Salts. Paper in Proceedings of the All-Union Conference on Physical Chemistry of Molten Salts and Slags (Nov. 22-25, 1960). Engl. Transl. AEC-tr-5948, Oct. 1983, pp. 207-214.

☆ U.S. GOVERNMENT PRINTING OFFICE: 1986—605-017/40,012

INT.-BU.OF MINES,PGH.,PA. 28211